The Development and Characterization of 'Rod-Hinge-Rod'-type Molecular Actuators

by

Laura G. Belasco

B.S., University of Rochester, 2004

Submitted to the Graduate Faculty of

The University of Pittsburgh in partial fulfillment

of the requirements for the degree of

Master of Science

University of Pittsburgh

2007

UNIVERSITY OF PITTSBURGH

Faculty of Arts and Science

This document was presented

by

Laura G. Belasco

It was defended on

April 5th, 2007

and approved by

Prof. Tara Meyer, Associate Professor

Prof. Kazunori Koide, Assistant Professor

Thesis Advisor: Prof. Christian Schafmeister, Assistant Professor

The Development and Characterization of 'Rod-Hinge-Rod'-type Molecular Actuators

Laura G. Belasco, M.S

University of Pittsburgh, 2007

We have successfully synthesized a bivalent hinged molecule that binds metal to undergo large conformational changes, similar to an actuator. Spectrophotometric titrations as well as a Job plot have shown that binding occurs on a 1:1 ratio of metal to hinged molecule. Addition of EDTA as a metal scavenger causes the molecule to return to the unbound state. Gel filtration chromatography has shown the effects of metal binding on the overall size and shape of the actuator molecule; the "closed" form is much smaller than the "open" form, indicating that large conformational changes are occurring upon binding. Analytical ultracentrifugation has unambiguously confirmed that the molecules are binding metal in a monomeric fashion.

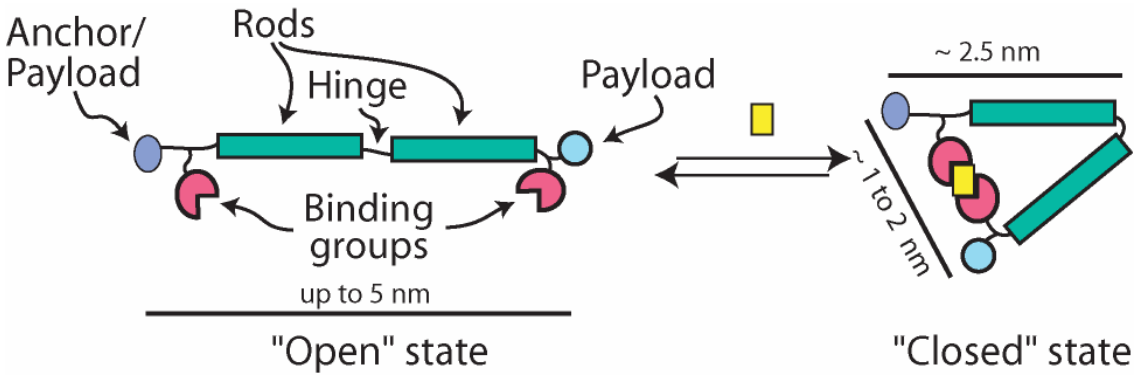

TABLE OF CONTENTS

LIST OF FIGURES

LIST OF SCHEMES

LIST OF ABBREVIATIONS

Ac	Acetyl
Boc	*t*-Butoxycarbonyl
DCM	Dichloromethane
DIPEA	Diisopropylethylamine
DMF	Dimethylformamide
Cbz	Carbobenzyloxy
EDTA	Ethylenediaminetetraacetic acid
HATU	*O*-(7-azabenzotriazon-1-yl)-*N,N,N',N'*-tetramethyluronium hexafluorphosphate
MSNT	1-(Mesitylene-2-sulfonyl)-3-nitro-1H-1,2,4-triazole
Q	8-Hydroxyquinoline
Q_A	8-Hydroxyquinolyl acetic acid
TFA	Trifluoroacetic acid

1.0 INTRODUCTION

Nanoscience is the study of all things on the nanometer scale (in the 1-100 nm range). It encompasses almost all disciplines in science and technology and involves imaging, measuring, modeling, and manipulating matter with atomic precision at this small scale.

Nature is one of the most complex and prolific makers of nano-scale machines. Billions of years of evolutionary feedback have produced extremely sophisticated and efficient biological machines. For example, enzymes have the ability to specifically produce and cleave chemical bonds, DNA stores information, and muscles can expand by the action of miniature motors. One example of nature's wonders is the bacterial flagellar motor.[1] The flagellar motor is only 50 nm in diameter, but its spinning can reach speeds on the order of 100 Hz. With the ability to move in any direction, coupled with receptors on the cell's surface to detect sugars or amino acids, cells can move to a more hospitable location. While the flagellar motor is incredibly complex, the basic parts are easier for scientists to emulate. The ability to create rotors, gears, and other basic devices artificially in the lab is the first step toward artificial molecular machines.

It is hoped that in the future, nanotechnology will provide pathways to molecular fabrication that rival nature in their elegance and efficiency.

---

[1] Berg, H. *Annular Review of Biochemistry*, **2003**, *72*, 19-54.

1.1 INTRODUCTION TO NANOTECHNOLOGY

The continued advancement of civilization hinges on our ability to create new and useful devices. In the past few decades, science has focused on making existing devices smaller, lighter, and faster. Some of the biggest advances in nanotechnology have come from the semiconductor industry. The ability to mass-produce improved devices for computers allows for more memory to be stored in the same amount of space, making smaller, faster and lighter machines possible. The current norm in manufacturing and miniaturization has been the "top-down" approach, where small materials are produced from larger structures. Microchips are generally produced using a top-down process known as photolithography[2], where a UV light is projected through a patterned mask onto a piece of silicon covered with a photosensitive film. After the film has been developed, areas that were exposed to light have been removed, and areas that were unexposed to light are intact, creating a detailed pattern on the surface of the microchip. Using this method, chips can be made as small as 100 nm; however, continued miniaturization will soon encounter the fundamental limitations set by the materials used.

One of the ways to keep up with this miniaturization trend to make smaller and smaller devices is to employ the "bottom-up" approach. This approach, which was originally proposed in 1959 by Richard Feynman[3], focuses on creating devices by assembling them one atom or

---

[2] "The History of the Integrated Circuit" www.nobelprize.org

[3] Feynman, R., "There's Plenty of Room at the Bottom," a talk at the annual meeting of the American Physical Society at CalTech, 12/29/59.

molecule at a time. The most popular of the bottom-up nanotechnology currently being studied includes quantum dots and nanotubes. [4,5,6,7]

In the future, it is hoped that nanotechnology will enable the development of nanoscale machines capable of systematically manufacturing large-scale atomically precise products cheaply and cleanly. These sorts of developments, as well as the possibilities that we cannot predict today, have the ability to improve medicine, the economy, and the environment.

1.2 NANOTECHNOLOGY AND MOLECULAR MACHINES

Although traditional synthetic chemistry (the manipulation of single atoms and functional groups) is a powerful tool for small molecules, there are many limitations, most notably poor overall yields and immense complexity. In order to produce large and complex nanoscale devices, different and more promising approaches need to be explored.

Rather than manipulate one atom at a time, supramolecular chemistry explores the manipulation of entire molecules. Supramolecular chemistry is eloquently defined by J.-M. Lehn as "the chemistry beyond the molecule, bearing on organized entities of higher complexity

---

[4] Cao, G. *Nanostructures & Nanomaterials: Synthesis, Properties & Applications,* Imperial College Press, London, 2004.

[5] Bowers, M.J.; McBride, J.R.; Rosenthal, S.J. *J. Am. Chem. Soc.* **2005**, *127*, 15378 – 15379.

[6] Iijima, S. *Nature*, **1991,** *354,* 56-58.

[7] (a) Berber, S.; Kwon, Y.-K.; Tománek, D. *Phys. Rev. Lett*. **2000**, *84*, 4613-4616. (b) Kociak, M.; Kasumov, A.Yu.; Guéron, S.; Reulet, B.; Khodos, I.I. Gorbatov, Yu.B.; Volkov, V.T.; Vaccarini, L.; Bouchiat, H. *Phys. Rev. Lett.* **2001**, *86*, 2416-2419.

that result from the association of two or more chemical species held together by intermolecular forces."[8] While traditional organic chemistry involves forming and cleaving covalent bonds, supramolecular chemistry makes use of noncovalent interactions, which are much weaker and often reversible, including hydrogen bonding, metal coordination, and electrostatic effects to assemble molecules into multi-molecular complexes.

The construction of rotors and other devices is often accomplished using the principles of supramolecular chemistry. Molecular rotors usually involve free rotation around bonds. One such rotor can be found in the metal *bis*-(porphyrinate) double-decker compounds (Scheme 1).[9] When seen from the top, they can be viewed as two overlapping wheels that rotate about a molecular axle.

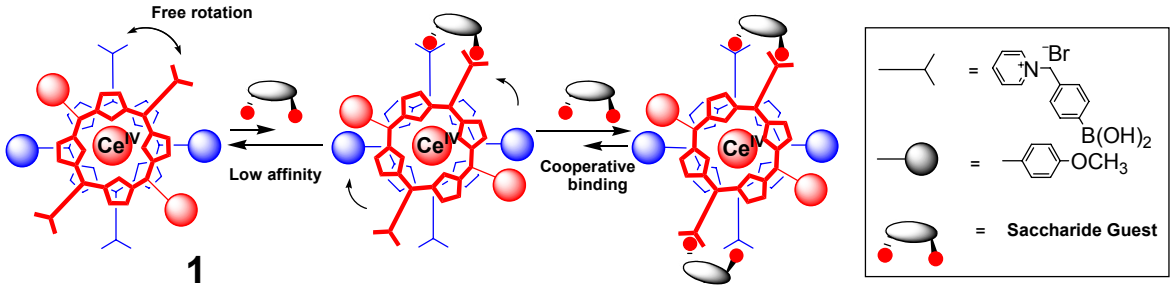

Scheme 1: Cooperative binding of saccharides in a molecular rotor.

The porphyrin complex (**1**) has free rotation, using the cerium bonds as an axle. However, as a saccharide guest molecule is bound, a positive allosteric affect induced by the

[8] Lehn, J.-M. *Angew. Chem. Int. Ed. Engl.* **1988**, *27*, 89.

[9] (a) Tashiro, K.; Konishi, K.; Aida, T. *Angew. Chem. Int. Ed. Engl.* **1997**, *36*, 856-858. (b) Shinkai, S.; Ikeda, M.; Sugasake, A.; Takeuchi, M. *Acc. Chem. Res.* **2001**, *34*, 494-503.

interaction results, and a loss of rotation occurs, which can be regarded mechanically as a "braking" effect.

Not only can molecular machines be based on rotation about a metal-ligand coordination bond like the porphyrin rotor, but they can be based on chemical reactions which produce movement. These include isomerization reactions, acid-base or redox reactions that make or break covalent or hydrogen bonds, and metal-ligand reactions that make or break coordination bonds.

A recent and novel molecular device using an isomerization reaction to cause movement involves "precipitons" developed by Wilcox.[10] These molecules are based upon the structure of stilbene, which can exist in two different isomerization forms, *cis* (**2**) and *trans* (**3**). Because the *cis* form is much more soluble in a given solvent than the *trans* form, an isomerization reaction can allow for the easy separation of these molecules from a reaction mixture.

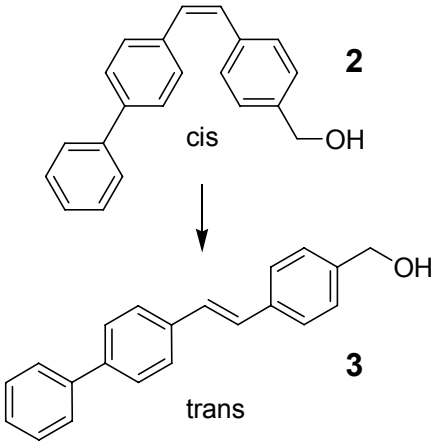

Figure 1: Stilbene-based Precipitons.

[10] Bosanac, T.; Yang, J.; Wilcox, C.S *Agnew. Chem.* **2001**, *133*, 1927-1931.

When relevant functional groups are appended, these precipitons have been proven to work as scavengers in copper catalyst removal (Figure 2).[11] In this case, UV radiation is the *cis* to *trans* trigger that causes the metal-precipiton complex to fall out of solution.

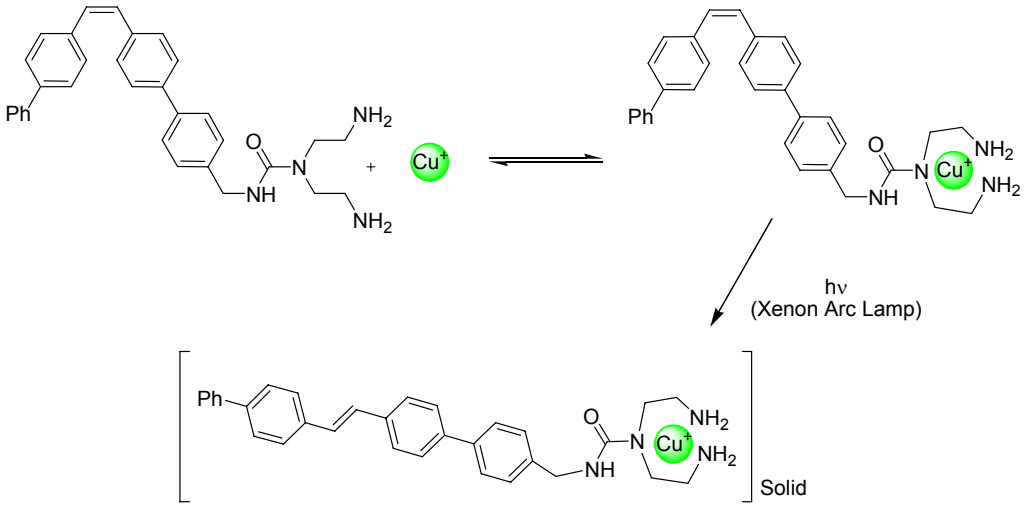

Figure 2: Metal-scavenging precipitons.

A few systems that use acid-base reactions to produce movement are [2]rotaxanes and catenanes. In these cases, while the two components are not linked covalently, they cannot dissociate from one another either. Their molecular motions are based upon either the rotation of the macrocycles, or the movement of the macrocycle from one site to another on the dumbbell-shaped molecules (Figure 3). By controlling the movement of the macrocycles, with either hydrogen- or metal-binding sites, they can function as molecular switches or shuttles with potential uses in molecular electronics as logic switching elements.[12]

---

[11] Honigfort, M.; Brittain, W. J.; Bosanac, T.; Wilcox, C. S. *Macromolecules* **2002**, *35*, 4849.

[12] Sauvage, J.-P. *Acc. Chem. Res*. **1998**; *31*, 611-619.

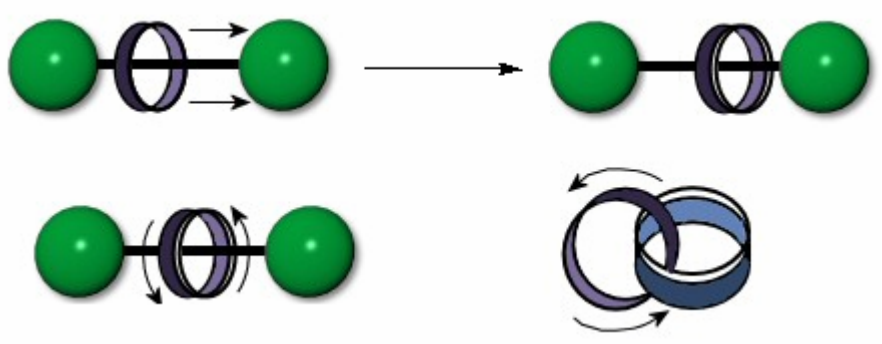

Figure 3: Schematic representation of the possible motions of rotaxanes and catenanes.

One of the most famous examples of rotaxanes as molecular devices is J.F. Stoddart's molecular elevator.[13] By using an interlocked three rotaxane system with different recognition sites and a three-ring macrocycle with different affinities for each recognition site, a stable, multivalent elevator was created. It was synthesized by threading the macrocyclic system (**4**) onto the rotaxane center (**5**), followed by stoppering the open ends (**6**) to lock the ring mechanically into place (Scheme 2). The ring system can be moved from one site to the other by the addition of acid or base.

[13] (a) Badjic, J.D.; Balzani, V.; Credi, A.; Stoddart, J.F. *Science* **2004**, *303*, 1845-1849. (b) Badjic, J.D.; Ronconi, C.M.; Stoddart, J.F.; Balzani, V.; Silvi, S.; Credi, A. *J. Am. Chem. Soc.* **2006**, *128*, 1489-1499.

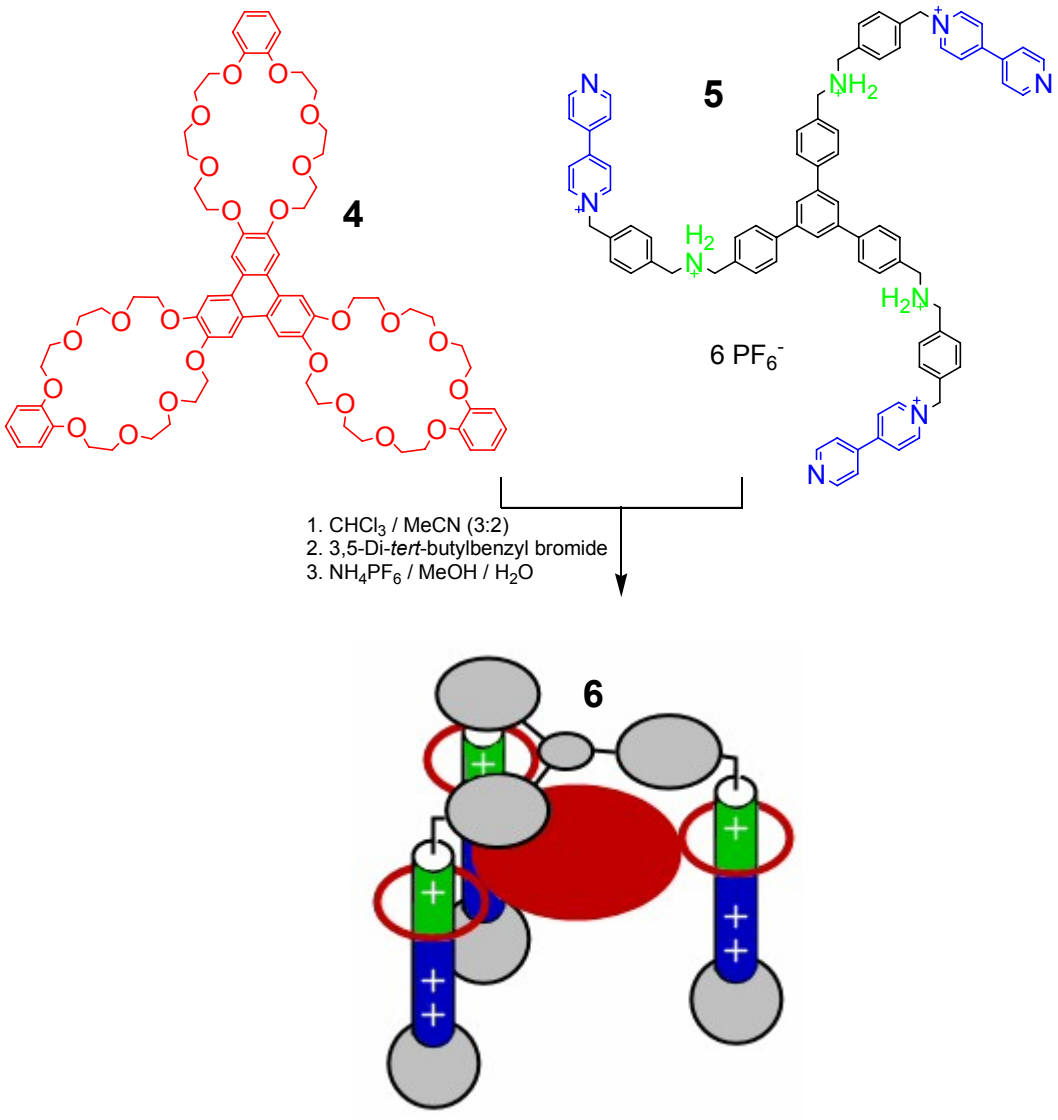

Scheme 2: Molecular elevator synthesis.

Although the most complex molecular machines being studied today are not on the level of those made by nature, the ability to understand and mimic nature is the first step toward creating synthetic devices that can compete side-by-side with those made by nature.

1.3 FOLDAMERS AND THE ROLE OF *BIS*-AMINO ACIDS

The functionality exhibited by proteins in nature is based on their three-dimensional structures. Something that has long eluded biochemists is the ability to predict how a protein can reliably fold from a primary sequence of amino acids monomers into a single, stable tertiary structure despite almost infinite possibilities. The folding is directed by various interactions such as hydrogen bonding, van der Waals forces, and dipole interactions, the combination of which has so far been impossible to predict for an artificial biomolecule. This is known as the protein-folding problem and it has obstructed the creation of useful synthetic proteins.

Foldamers are one way scientists are trying to get around the protein folding problem. Foldamers are a class of unnatural oligomers that mimic proteins and other biomolecules by folding into well-defined secondary structures using only non-covalent interactions such as hydrogen bonding, π-stacking, etc.

Foldamers have demonstrated the ability to perform many functions, including self-assembly, host-guest chemistry, and molecular recognition.[14] They are a useful alternative to supramolecular assemblies due to their versatility and ease of construction from monomers. Several examples of monomers that have been used in foldamers are shown in Figure 4.[15]

---

[14] Hill, D.J.; Mio, M.J.; Prince, R.B.; Hughes, T.S.; Moore, J.S. *Chem. Rev.* **2001**, *101*, 3893-4011.

[15] (a) Seebach, D.; Abele, S.; Sifferlen, T.; Hänggi, M.; Gruner, S.; Seiler, P. *Helv. Chim. Acta* **1998,** *81,* 2218-2243. (b) Appella, D.H., Barchi, J.J.; Durell, S.R.; Gellman, S.H. *J. Am. Chem. Soc.* **1999,** *121*, 2309-2310. (c) Kirshenbaum, K.; Barron, A.E.; Goldsmith, R.A.; Armand, P.; Bradley, E.K.; Troung, K.T.V.; Dill, K.A.; Cohen, F.E.; Zuckermann, R.N. *Proc. Natl. Acad. Sci. U.S.A.* **1998**, *95*, 4303-4308. (d) Claridge, T.D.W., Long, D.D.; Hungerford, N.L.; Aplin, R.T.; Smith, M.D.; Marquess, D.G.; Fleet, G.W.J. *Tetrahedron Lett.* **1999**, *40*, 2199-2202. (e) Smith, A.B.; Guzman, M.C.; Sprengeler, P.A.; Keenan, T.P.; Holcomb, R.C.; Wood, J.L.; Carroll, P.J.;

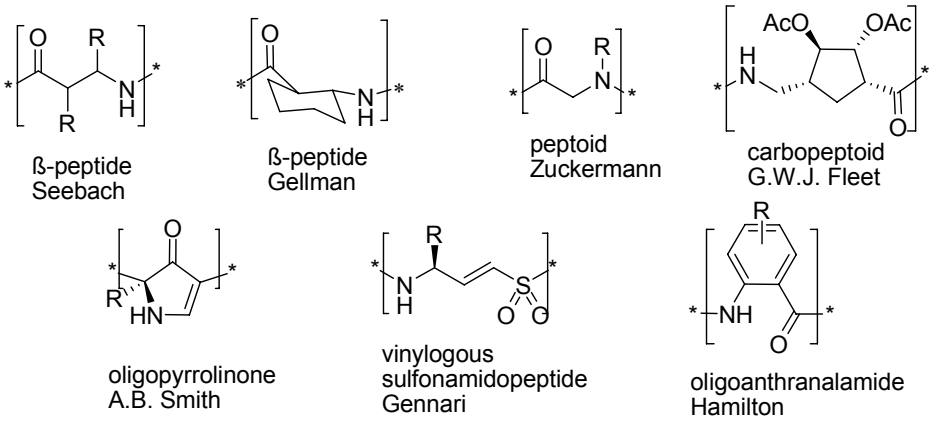

Figure 4: Examples of current foldamers.

One example uses Moore's water-soluble *m*-phenylene ethynylene monomer (Figure 5).[16] The use of hexaethylene glycol side chains increases solubility of the foldamer and the hydrophobic interior creates a pocket in which small molecules can bind. Seen below in Figure 5 is the binding of the foldamer with (-) α-pinene.

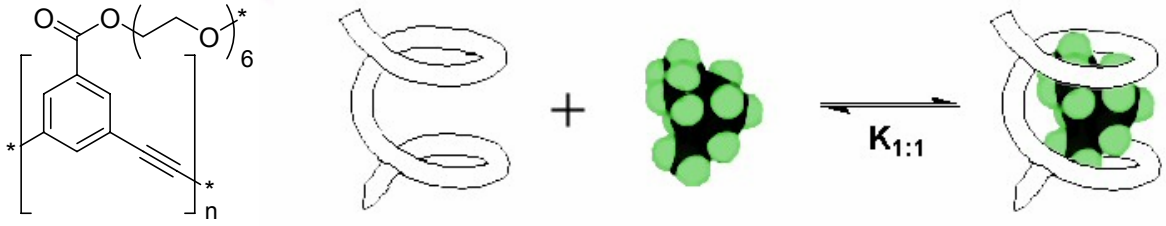

Figure 5: The monomer used; The binding of a small molecule in the foldamer.

Hirschmann, R. *J. Am. Chem. Soc.* **1994**, *116*, 9947-9962. (f) Gude, M.; Piarulli, U.; Potenza, D.; Salom, B.; Gennari, C., *Tetrahedron Lett.* **1996**, *37*, 8589-8592. (g) Hamuro, Y.; Geib, S.J.; Hamilton, A.D. *J. Am. Chem. Soc.* **1996**, *118*, 7529-7541.

[16] Stone, M.T.; Moore, J.S. *Org. Lett.* **2004**, *6*, 469-472.

Another approach to biomimetic molecules pioneered by the Schafmeister group[17] is the use of *bis*-amino acids as monomers in the synthesis of water-soluble oligomers. These *bis*-amino acids couple to each other through pairs of amide bonds to form spiro-ladder oligomers (Figure 6). These oligomers do not fold, rather they display complex shapes due the conformational preferences of the fused ring systems as well as the inherent stereochemistry of the monomers.

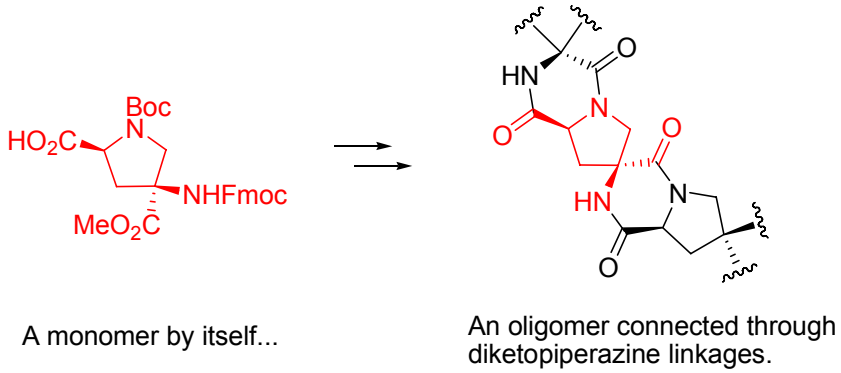

Figure 6: A monomer & its corresponding fused ring system counterpart.

The continuing goal of our group is to be able to create functional oligomers by programming a specific sequence from our current library of monomers to create different three-dimensional shapes (Figure 7).

---

[17] (a) Levins, C.G.; Schafmeister, C.E. *J. Am. Chem. Soc*. **2003**, *125*, 4702-4703. (b) Habay, S.A,; Schafmeister, C.E. *Org. Lett.* **2004**, *6*, 3369-3371. (c) Gupta, S.; Das, B.C.; Schafmeister, C.E. *Org. Lett.* **2005**, *7*, 2861-2864. (d) Levins, C.G.; Schafmeister, C.E. *J. Org. Chem.* **2005**, *70*, 9002-9008. (e) Levins, C.G.; Brown, Z.Z.; Schafmeister, C.E. *Org. Lett.* **2006**, *8*, 2807-2810.

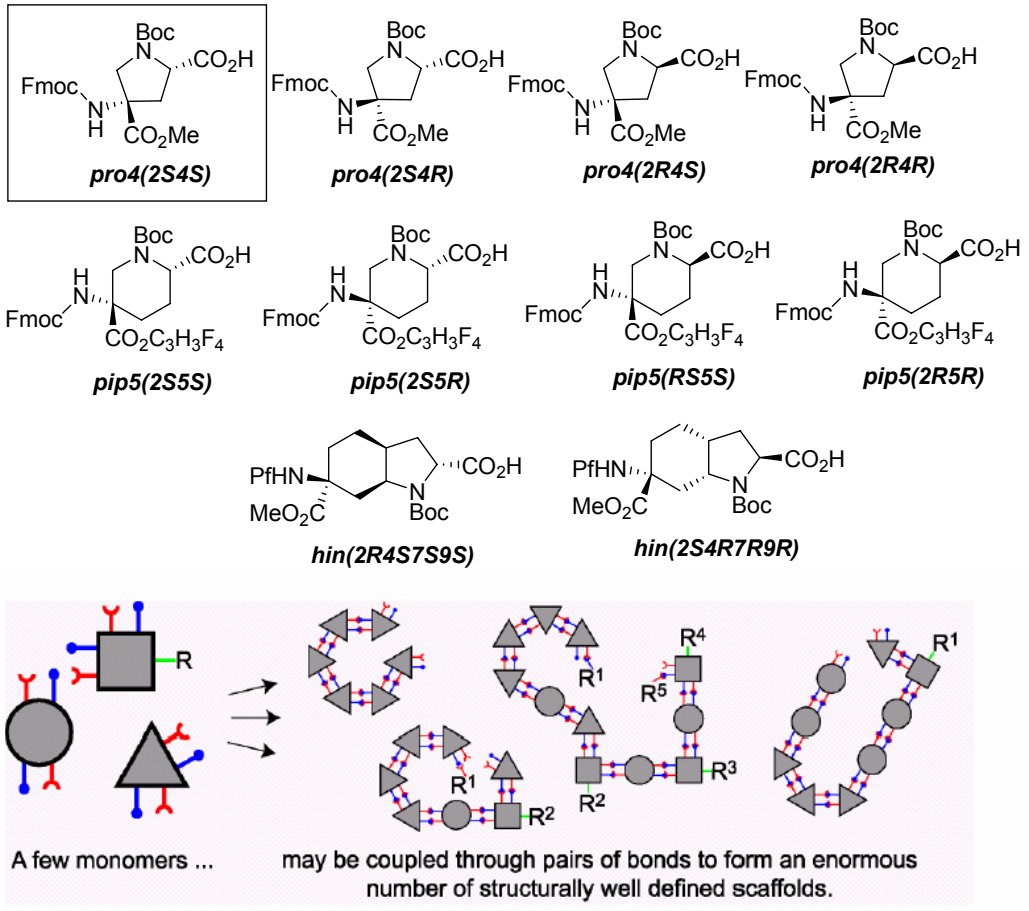

Figure 7: The library of monomers and a representation of possible complex shapes.

As we are still working toward this goal of creating complex shapes and functionalities, we seek to use our most common monomer, the pro4(2*S*4*S*) monomer, to create a basic molecular machine. An oligomer consisting of consecutive pro4(2*S*4*S*) monomers coupled together creates a simple rod.[18] We want to use simple components: two rods, a hinge, and metal-binding receptors, to create something more complex, a molecular device.

[18] Levins, C.G.; Schafmeister, C.E. *J. Am. Chem. Soc.* **2003**, *125*, 4702-4703.

2.0 MOLECULAR ACTUATORS CONTROLLED BY METAL BINDING

We seek to develop a molecular machine that can exist in two different states, and with the ability to move payloads long distances, i.e. ~3 nm, using a single variable – the presence or absence of metal. A system such as this is known as an actuator: a device that transforms an input signal into motion.

With this in mind, we utilized 8-hydroxyquinoline (**Q**) in our bis-amino acid oligomer system. We created an oligomer with a rod-hinge-rod assembly that can display different payloads on either side, and placed a **Q** at each end as a metal binding group (see Figure 8).

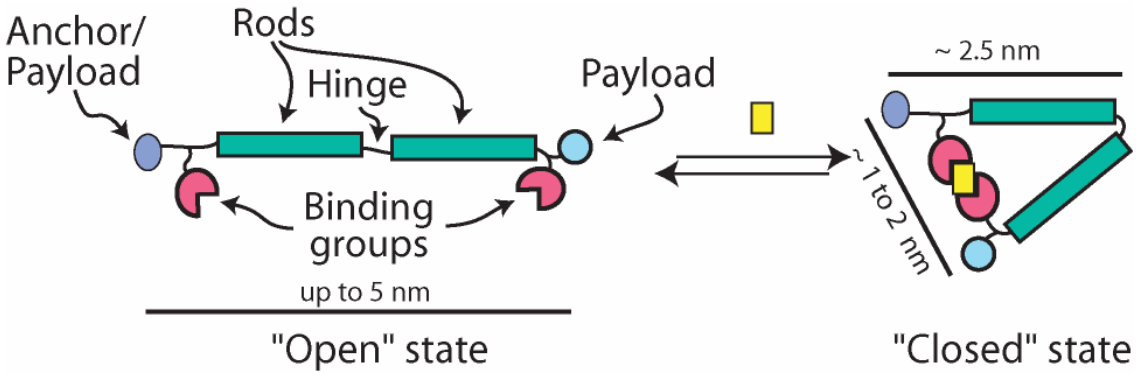

Figure 8: Molecular actuator in open and closed states.

In the absence of metal, the oligomer should be extended and floppy (the "open" state) due to the rotatable bonds in the hinge, with an extended length of up to 5 nm. When metal is introduced however, we believe that the oligomer folds up into the "closed" state (~2.5 nm by ~1

to 2 nm), forming a 1:1 monomeric complex with the metal. With this system, in addition to the open/closed state we desire, there is also the possibility of dimerization, trimerization, etc. as well as aggregation of our oligomers in the presence of metal (Figure 9).

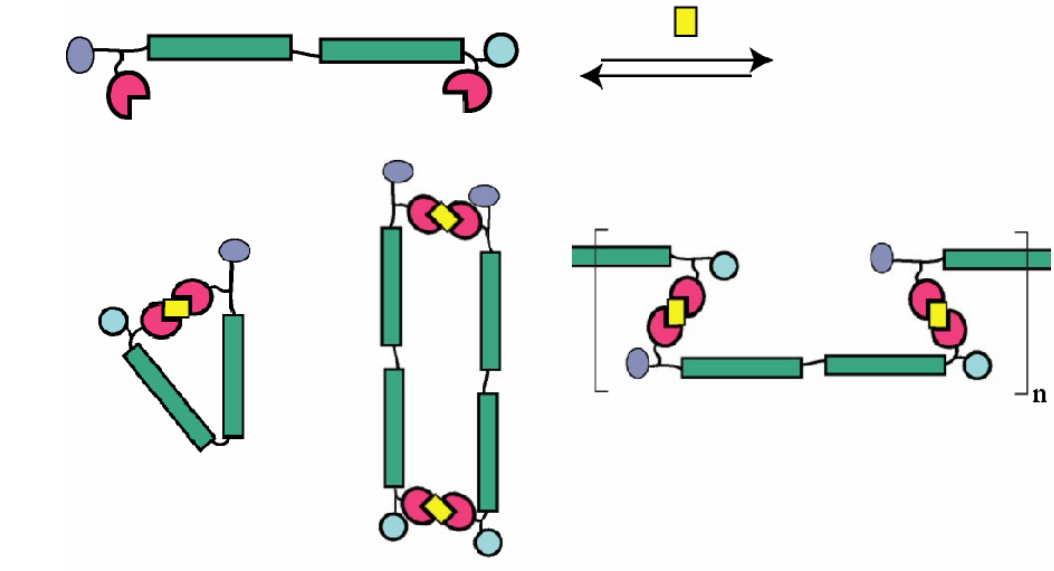

Figure 9: Possible bound conformations of the actuators: monomers, dimers, oligomers.

To characterize our assemblies, we have used UV/Vis spectroscopy, size-exclusion chromatography, and analytical centrifugation. Low solubility of these complexes in the presence of metals impeded our ability to study them using NMR.

2.1 8-HYDROXYQUINOLINE AS A MODEL SYSTEM

In order to study the binding and structural properties of our actuator, we decided to incorporate as the binding group an 8-hydroxyquinoline (**Q**) derivative. Its square planar structure[19] as well as its binding properties to various metals have been studied extensively, with copper being one of the most stable metals in the Mellor and Maley chelate stability series. [20] The overall association constant for copper binding to **Q** [$\mathbf{Q}_2$Cu] has been found to be approximately K = 8×10^{24} M^{-2},[21] which corresponds to a favorable free energy of ~33 kcal/mol at 25 ºC. When this is shown in comparison to a typical carbon-hydrogen bond strength of 81 kcal/mol,[22] it is seen that the 8-hydroxyquinoline [$\mathbf{Q}_2$:Cu] system is extremely tight binding. As a synthetic complex, 8-hydroxyquinoline is commonly used as a binding or molecular recognition tool.[23]

---

[19] (a) Bevan, J.A.; Graddon, D.P.; McConnell, J.F. *Nature (London)* **1963**, *199*, 373. (b) Murray-Rust, P.; Wright, J.D. *Inorg. Phys. Theor.* **1968**, 247-253. (c) Hoy, R.C.; Morriss, R.H.; *Acta Crystallogr.* **1967**, *22*, 476-482.

[20] (a) Schulman, S.G.; Gershon, H. *J. Inorg. Nucl. Chem.* **1969**, *31*, 2467-2476. (b) Näsänen, R.; Penttinen, U. *Acta Chem. Scand.* **1952**, *6*, 837-843. (c) Richard, C.F.; Gustafson, R.L.; Martell, A.E. *J. Am. Chem. Soc.* **1959**, *81*, 1033-1040. (d) Mellor, D.P.; Maley, L.E. *Australian J. Sci. Research* **1949**, *2A*, 92-110.

[21] Albert, A. *Biochem. J.* **1953**, *54*, 646-654.

[22] Huber, K.P; Herzberg, G., Molecular Spectra and Molecular Structure Constants of Diatomic Molecules, Van Nostrand, New York, 1979.

[23] (a) Watson, R.M.; Skorik, Y.A. Patra, G.K.; Achim, C. *J. Am. Chem. Soc.* **2005**, *127*, 14628-14639. (b) Asher, S.A.; Sharma, A.C.; Goponenko, A.V.; Ward, M.M. *Anal. Chem.* **2003**, *75*, 1676-1683.

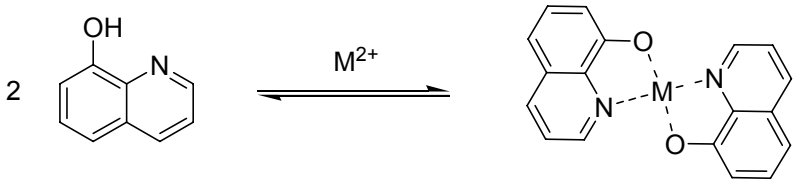

Figure 10: 8-hydroxyquinoline in its free and bound forms.

In order to attach it to our scaffolds as well as due to its low solubility in water, we decided to convert 8-hydroxyquinoline into the more soluble 8-hydroxyquinolyl acetic acid ($\mathbf{Q_A}$) derivative. This also allowed us to incorporate the binding group into our oligomers using solid phase synthesis. It was prepared as seen in Scheme 3, using literature procedures.[24]

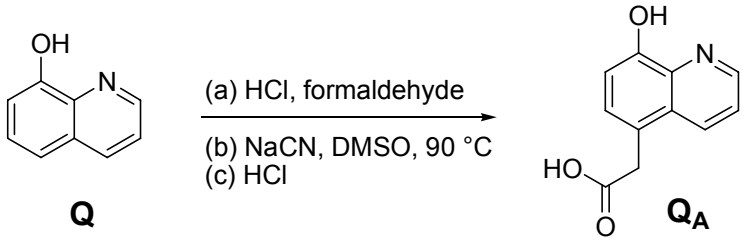

Scheme 3: Synthesis of 8-hydroxyquinolyl acetic acid.

In the UV-Vis absorption spectra of $\mathbf{Q_A}$ in pH 7.0 sodium phosphate buffer, the two strong absorption bands at 244 nm and 259 nm stand out strongly in the absence and presence of metal respectively. Weakly absorbing peaks are seen at 320 nm and 385 nm. Addition of metal causes absorption bands to red shift from 244 nm to 259 nm and 320 to 385 nm, demonstrating that metal binding to $\mathbf{Q_A}$ is occurring (Figure 11).

---

[24] (a) Burckhalter, J.H.; Leib, R.I. *J. Org. Chem.* **1961**, *26*, 4078-4083. (b) Warner, V.D.; Sane, J.N.; Mirth, D.B.; Turesky, S.S.; Soloway, B. *J. Med. Chem.* **1976**, *19*, 167-169.

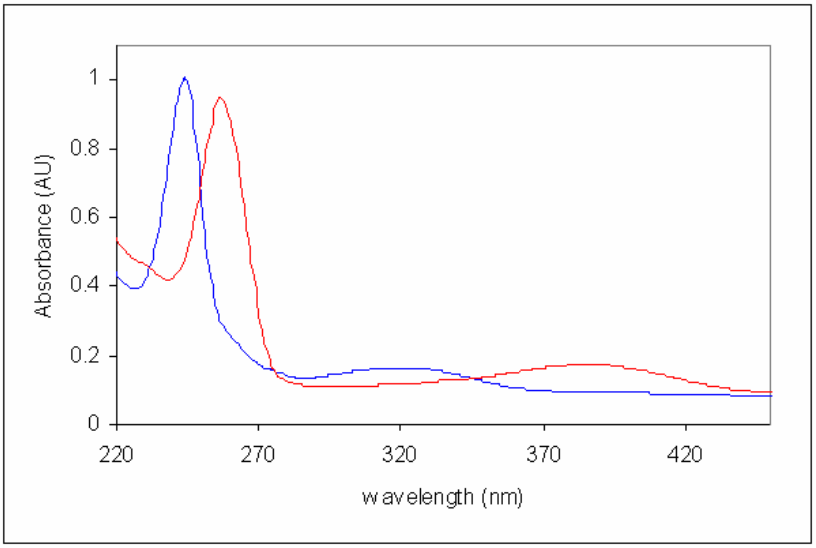

Figure 11: UV/Vis absorption, blue - unbound Q_A, red - Q_A bound to Cu.

A titration was performed using 22 μM **Q_A** by addition of small aliquots of 380 μM $CuCl_2$ in pH 7.0 phosphate buffer. The titration curves show an inflection point at Cu^{2+}:**Q_A** of ~1:2. Isosbestic points are observed at 251 nm and 346 nm, suggesting a direct conversion of one species to another, **Q_A** → [Q_{A2}:Cu] – 2:1 binding (Figure 12). Further addition of Cu^{2+} shows no other inflection points, indicating that once the 2:1 complex forms, it cannot be converted by excess Cu^{2+} to 1:1 complexes (Figure 13).

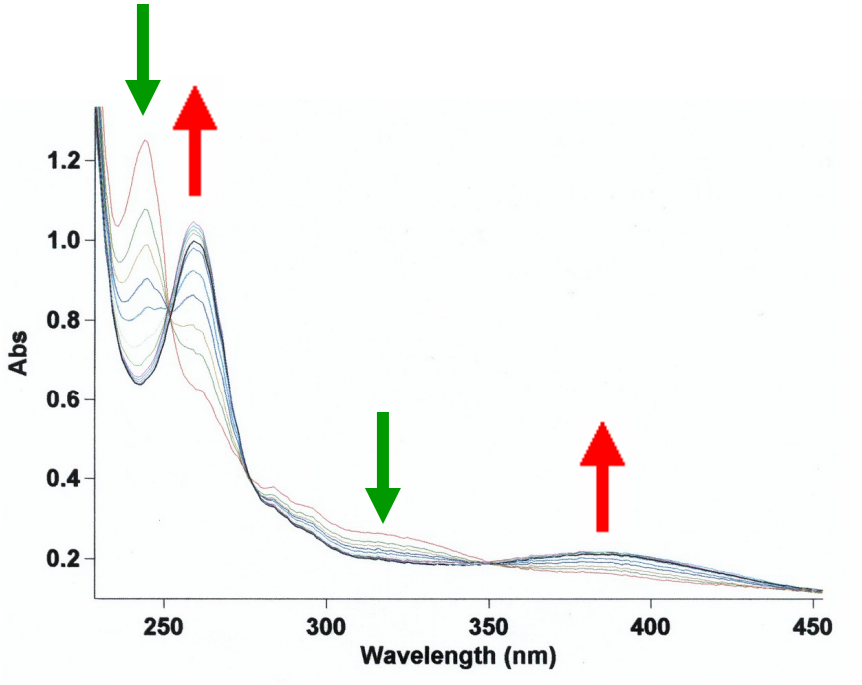

Figure 12: Spectrophotometric titration of a 22 µM solution of Q_A (10 mM sodium phosphate buffer, pH 7.0, T = 25 ºC) with a 380 µM solution of $CuCl_2$. The arrows indicate the direction of change in absorbance with increasing copper concentration.

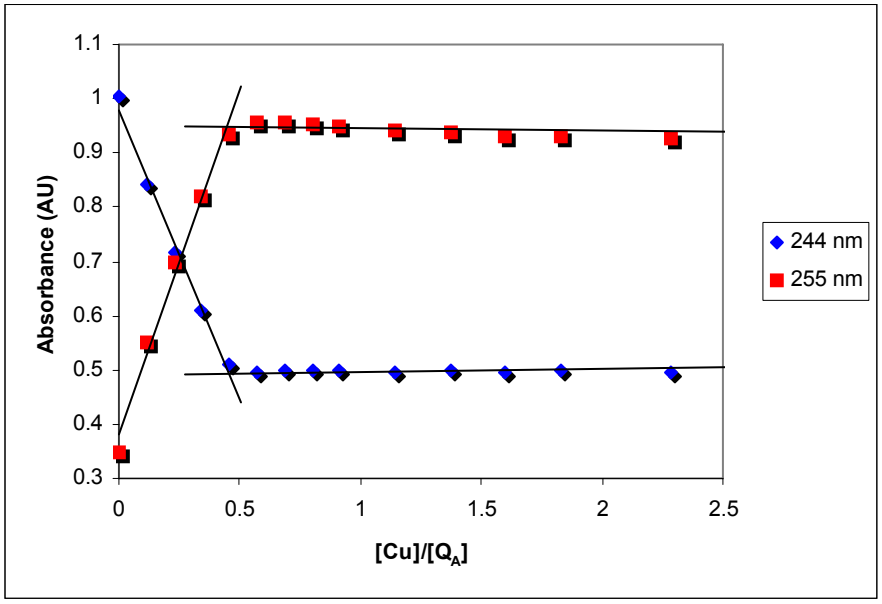

Figure 13: Spectrophotometric titration of Q_A, monitored at 244 nm and 259 nm (22 µM solution of Q_A, 10 mM sodium phosphate buffer, pH 7.0, T = 25 ºC, titrated with 380 µM $CuCl_2$).

2.2 ACTUATOR SYNTHESIS

Our initial design of the actuator had rods comprising of 4 building blocks, an (L)-ornithine hinge, and a napthylalanine chromophore: **7**.

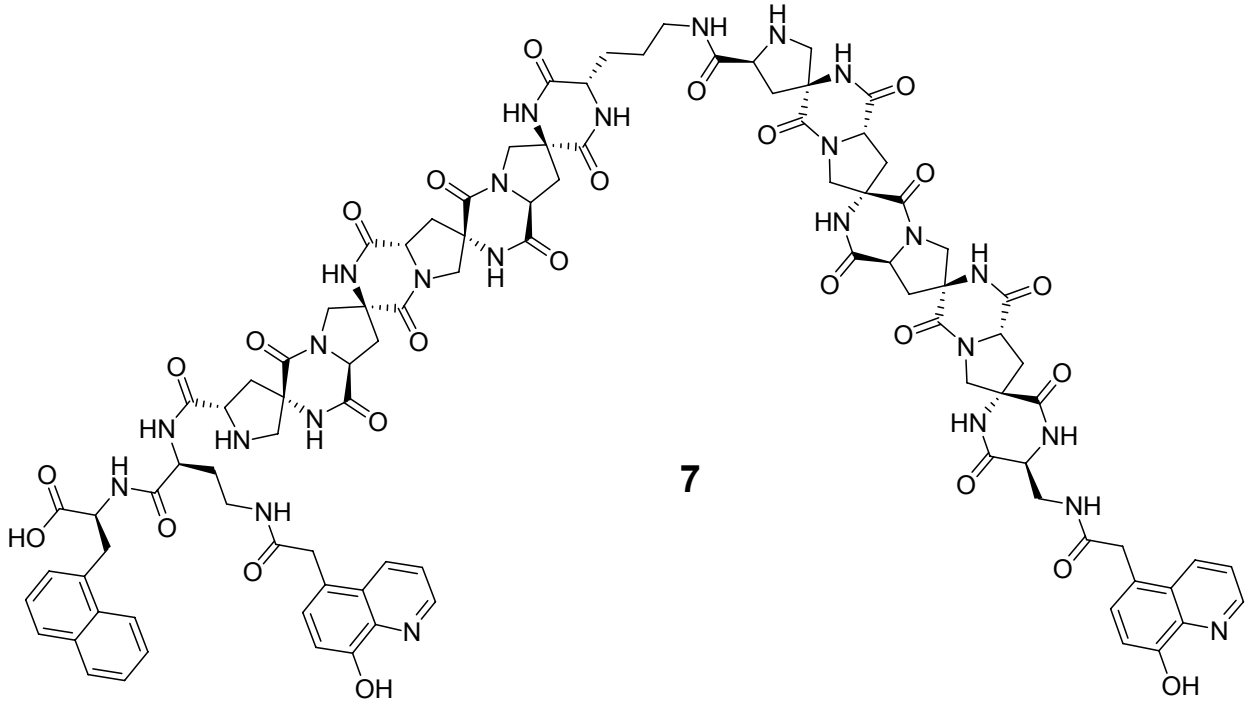

Figure 14: Scaffold structure of actuator 7.

Scaffold **7** was made using standard Fmoc solid phase peptide synthesis techniques. Fmoc-(L)-1-Napthylalanine, which provides a UV chromophore, was coupled initially (using MSNT and methyl imidazole) to the hydroxymethyl resin (**8**). An ivDde-protected diaminobutanoic acid group was coupled next using the standard HATU / DIPEA conditions to give compound **9**. This was followed by the coupling of four consecutive pro4(2S4S) monomers to form the first "rod" section of the actuator (**10**).

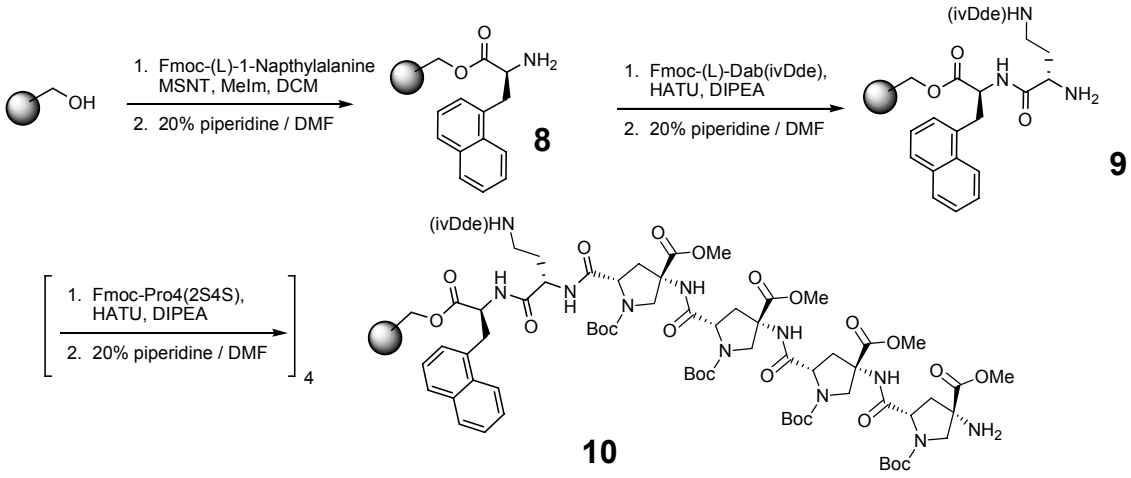

Scheme 4: Solid phase synthesis of scaffold 7.

Next, an Mtt-protected (L)-ornithine was attached for the "hinge" portion. Mtt deprotection, which does not remove the ivDde protected amine at the beginning of the rod, followed by another coupling of four consecutive pro4(2S4S) monomers formed the second "rod" section of the actuator (**12**).

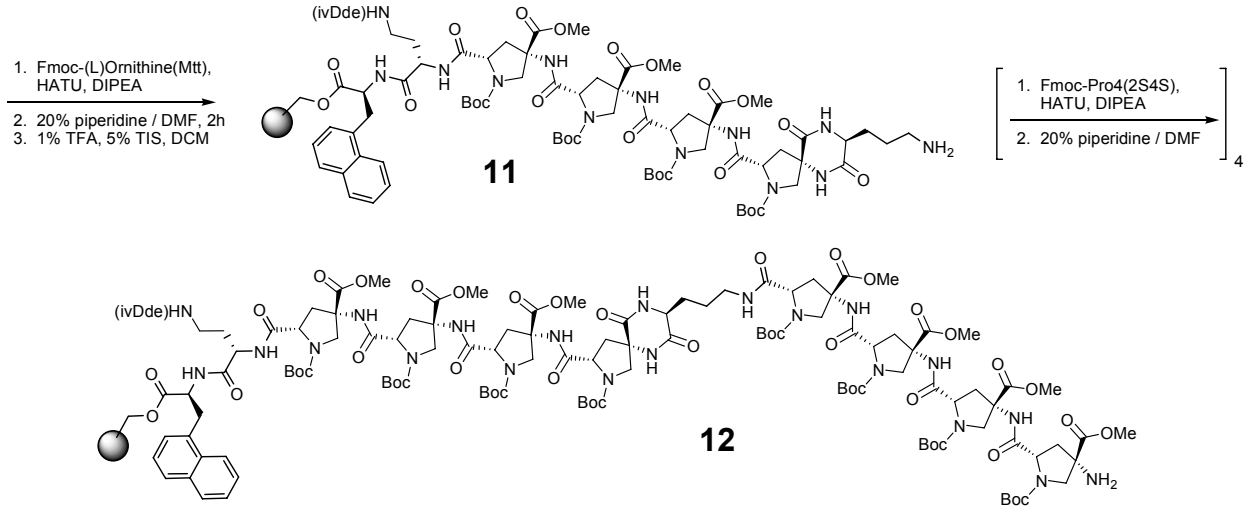

Scheme 5: Solid phase synthesis of scaffold 7.

Coupling of an Mtt-protected diaminopropionic acid followed by Mtt deprotection gave a free amine at the end of the scaffold. If another payload was desired at this end of the scaffold,

modifications at this point would be made for its inclusion. No end payload was required, so an ivDde deprotection allowed for the opening of the site at beginning of the molecule so the receptor can be coupled to both sites (**13**). Quadruple couplings with short 20% piperidine/DMF washings after each coupling, allowed for complete conversion to compound **14**, while preventing polymerization of $\mathbf{Q_A}$.

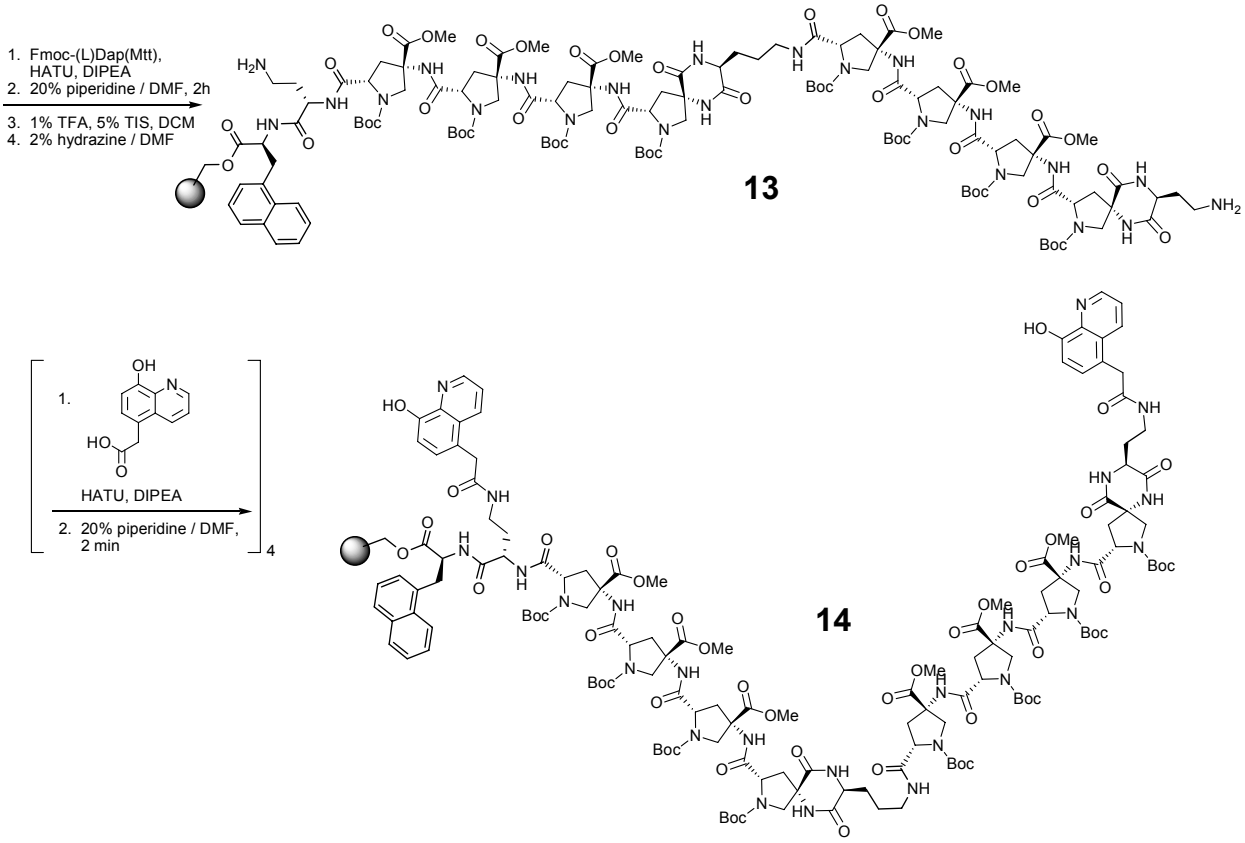

Scheme 6: Solid phase synthesis of scaffold 7.

Cleavage of the oligomer from the resin using standard triflic acid method was followed by base-catalyzed diketopiperazine (DKP) closure to give the final rigidified scaffold, **7**.

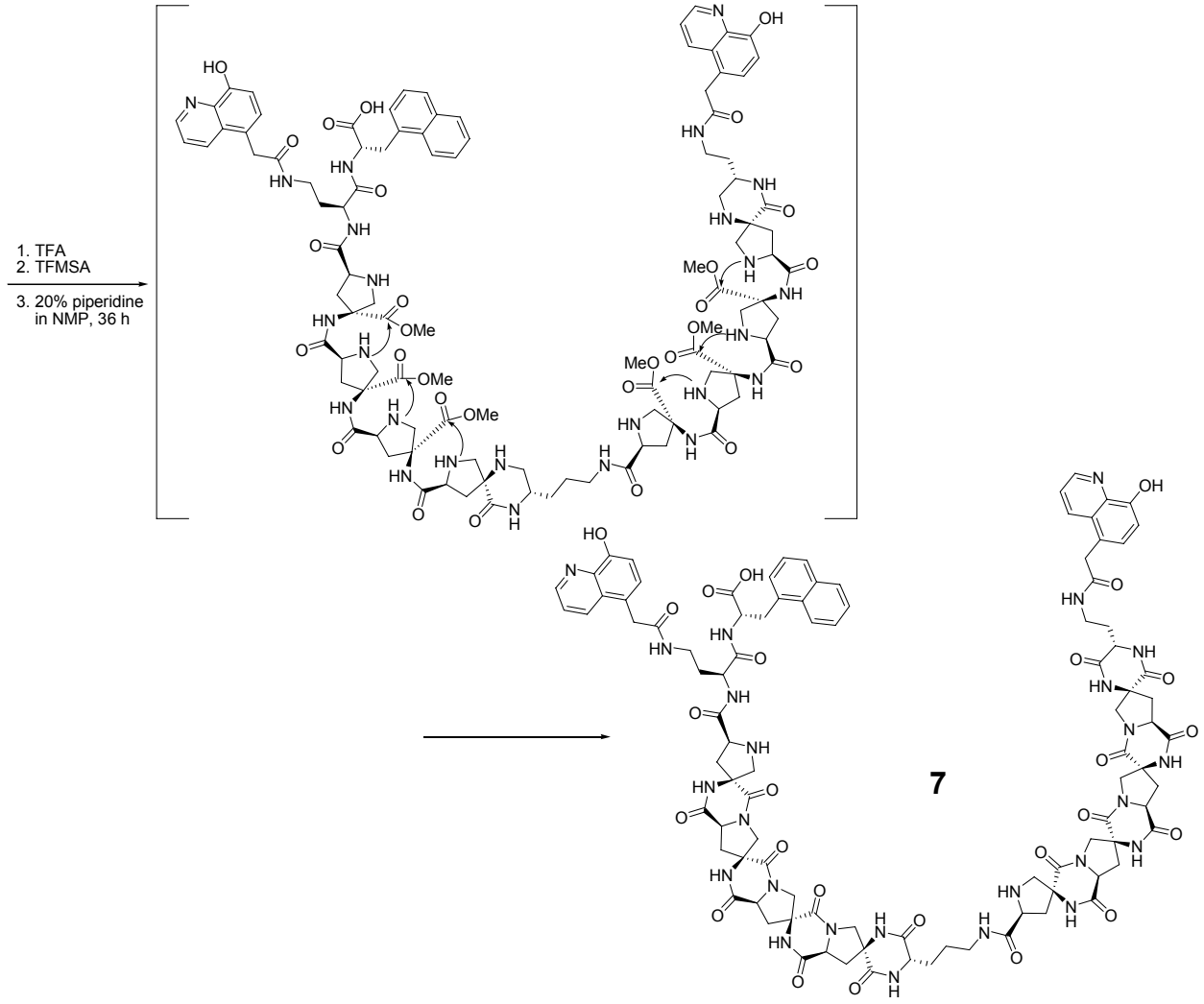

Scheme 7: Cleavage and DKP closure of scaffold 7.

2.3 RESULTS & DISCUSSION

The stoichiometry of Cu^{2+} binding to actuator **7** was studied by performing titrations and monitoring absorbance changes to the relevant wavelengths. A solution of scaffold **7** with a concentration of 17 μM was titrated with 150 μM $CuCl_2$ at room temperature (Figure 15).

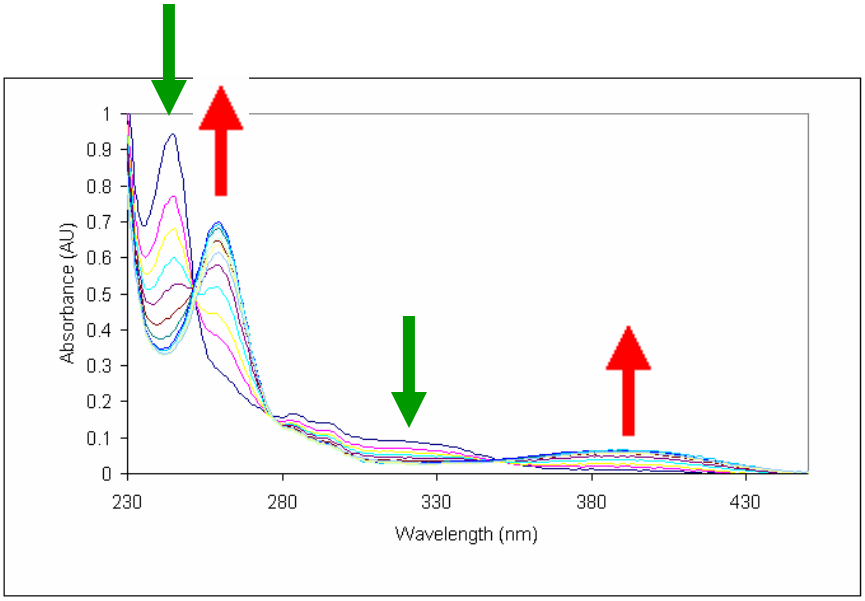

Figure 15: Spectrophotometric titration of a 17 µM solution of scaffold 7 (10 mM sodium phosphate buffer, pH 7.0, T = 25 ºC) with a 150 µM solution of $CuCl_2$. The arrows indicate the direction of change in absorbance with increasing copper concentration.

Isosbestic points are observed at 251 nm and 346 nm, suggesting a direct conversion of one species to another, **7** to [**7**:Cu] – 1:1 binding. The UV-Vis titration curves at 244 and 259 nm show an inflection point at Cu^{2+}:**7** of ~1:1. Further addition of Cu^{2+} shows no other inflection points, implying no formation of 1:2 (**7**:Cu_2) complexes (Figure 16).

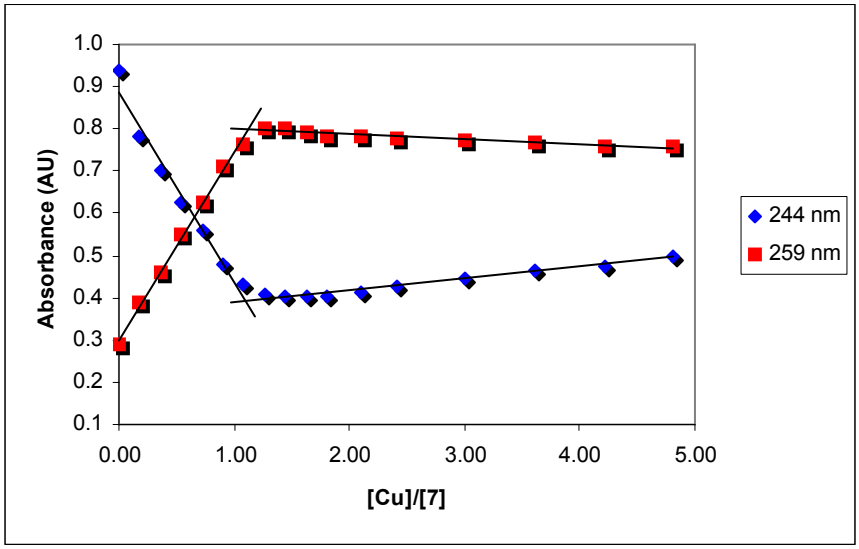

Figure 16: Spectrophotometric titration of 7 monitored at 244 nm and 259 nm (17 µM solution of 7, 10 mM sodium phosphate buffer, pH 7.0, T = 25 ºC, titrated with 150 µM $CuCl_2$).

Scaffold **7** was also titrated using other metals including $NiCl_2$, $CoCl_2$, $ZnBr_2$ with similar results to $CuCl_2$.

In addition to titrations, a Job plot experiment (Figure 17) was performed to confirm the stoichiometry of copper bound scaffold **7**.

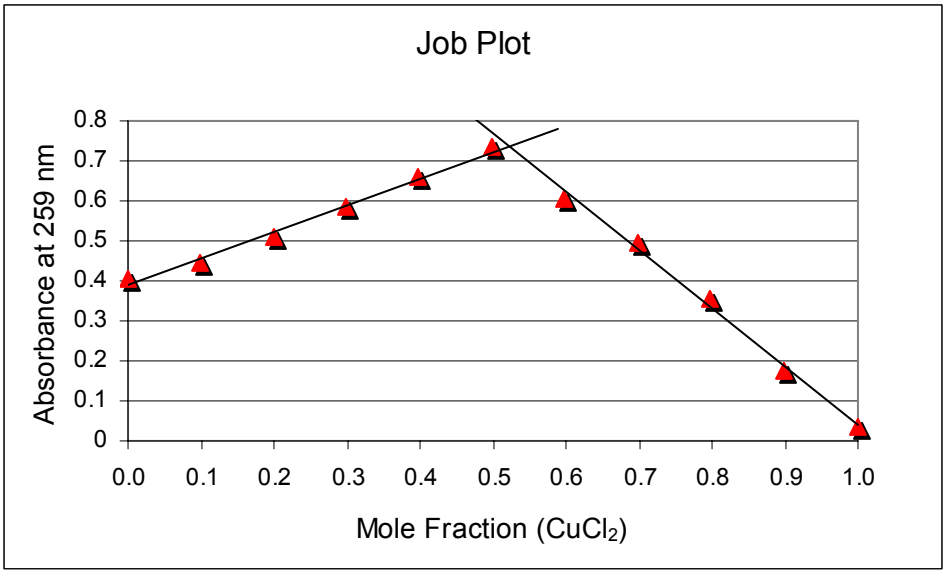

Figure 17: Job plot of scaffold 7 & $CuCl_2$.

As seen above, the Job plot shows a maximum at a mole fraction of approximately 0.52 indicating a 1:1 ratio of scaffold **7** to Cu^{2+}, confirming the stoichiometry findings from the copper titration.

The reversibility of the Cu^{2+} binding to scaffold **7** was studied using EDTA (ethylenediaminetetraacetic acid) as a copper scavenger. To a 27 μM solution of scaffold **7** at room temperature (a) was added 1 eq. $CuCl_2$ to fully bind all binding sites (b). Three equivalents EDTA was then added to scavenge the copper in solution. As seen in Figure 18, approximately 90-95% of scaffold **7** was returned to the unbound state with a λ_{max} of 244 nm (c).

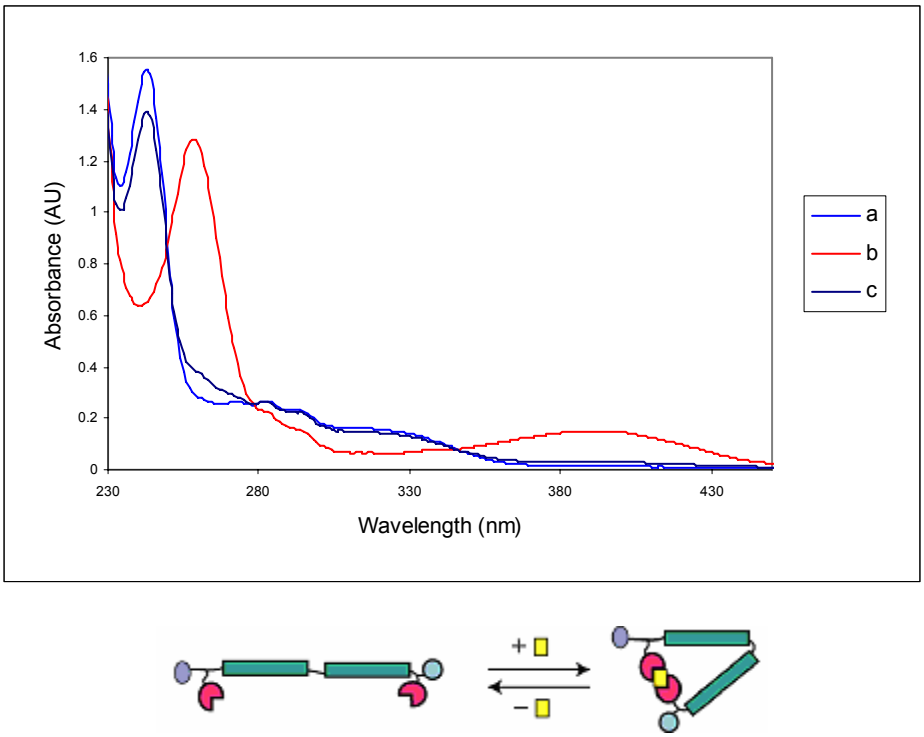

Figure 18: The reversibility of Actuator 7: (a) actuator sample with no metal present, (b) sample with one equivalent of $CuCl_2$ present, (c) sample after metal has been scavenged.

A hinge-less control molecule consisting of an 8 building block length rod, **15**, was synthesized and tested[25] to determine the stoichiometry of this molecule when monomeric actuation is impossible (Figure 19).

[25] Thanks to Sam Getchell for the synthesis and titration of molecule **15**.

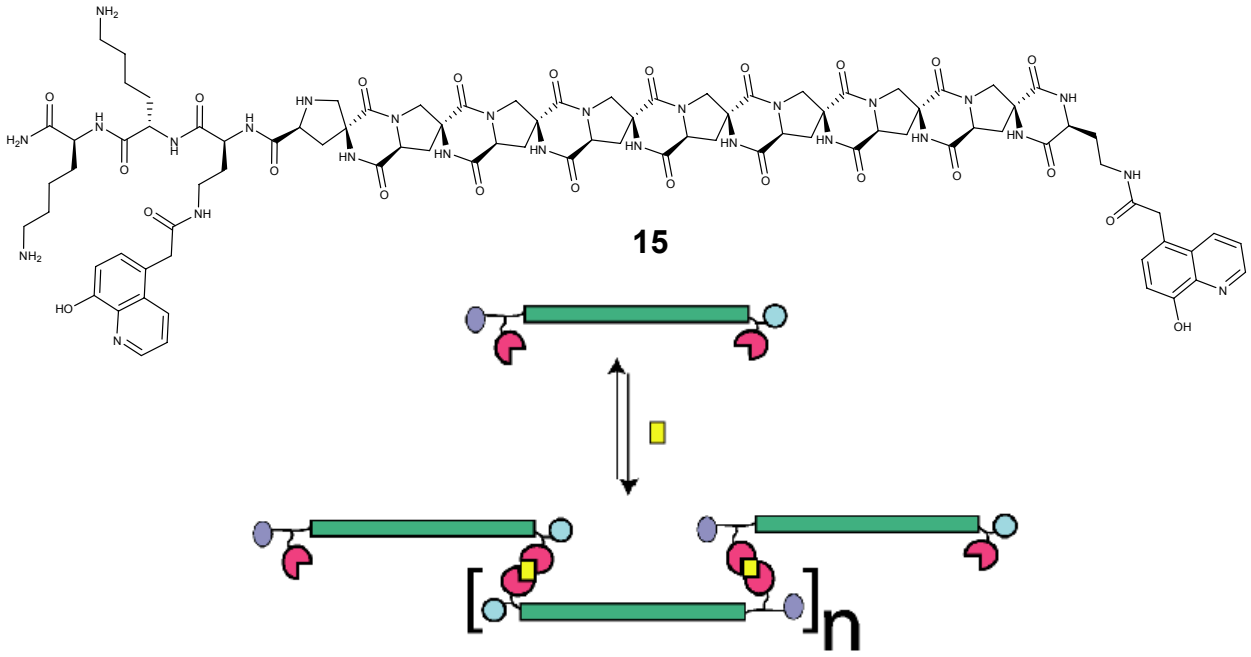

Figure 19: Scaffold 15.

UV/Vis experiments of this bivalent molecular rod were carried out by titrating a solution of 104 μM $CuCl_2$ into 18 μM **15** in a 7 mM pH 7.0 ammonium acetate / 30% acetonitrile solution (scaffold **15** was found to have poor solubility in phosphate buffer). As with scaffold **7**, the unbound state has peaks at 244 nm and 315 nm, characteristic of unbound $\mathbf{Q_A}$ (Figure 20). As metal is titrated in, peaks at 259 nm and 385 nm begin to appear, but then immediately disappear as more metal is added. This is also accompanied by a slight cloudiness to the titration solution. We believe that this indicates the molecule is binding metal and coordination polymers are forming which are so large that they precipitate out of solution.

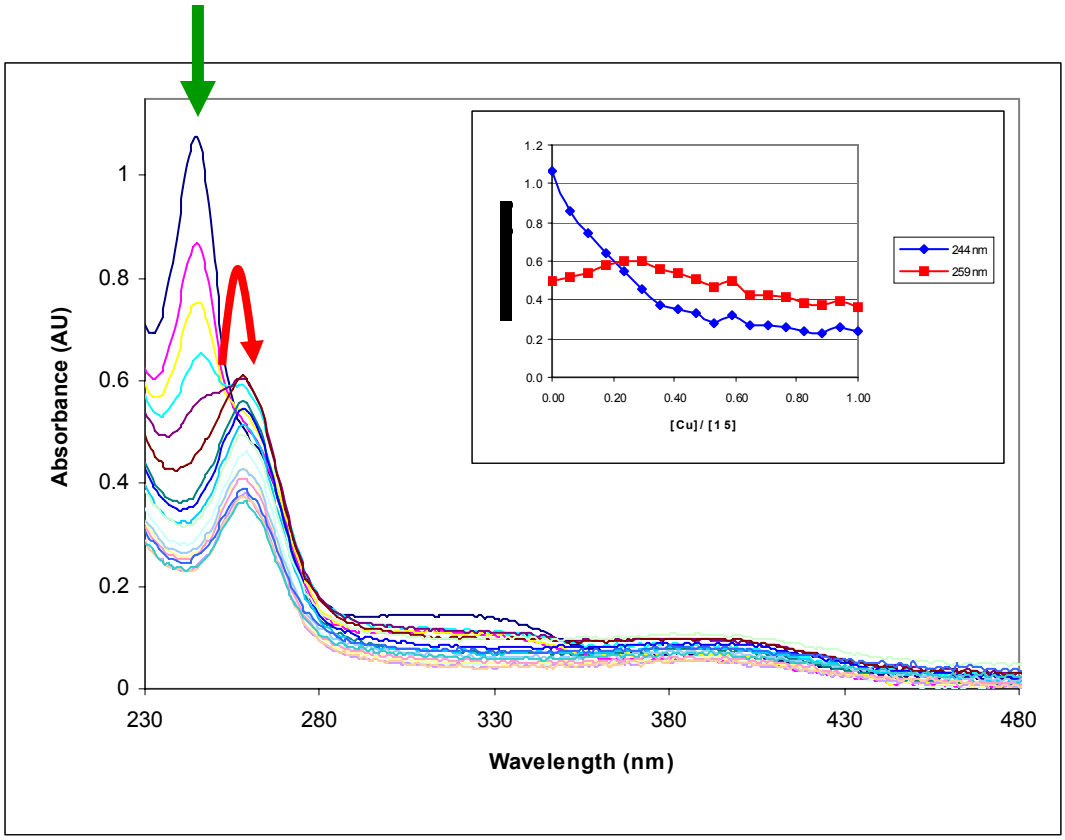

Figure 20: Spectrophotometric titration of an 18 µM solution of 15 (7 mM pH 7.0 ammonium acetate / 30% acetonitrile buffer solution, pH 7.2, T = 25 ºC) with 104 µM $CuCl_2$. Inset are the corrected titration curves, monitored at 244 nm and 259 nm.

Gel filtration chromatography (also known as size exclusion chromatography) is a technique in which compounds are separated based on their size rather than affinity with the column matrix. The column matrix is a composite of cross-linked agarose and dextran, a porous media in the form of spherical particles. As the buffer and sample move through the column, molecules diffuse in and out of the pores of the column matrix. Small molecules can diffuse further into the pores and migrate slowly, while molecules that are larger than the pores of the matrix cannot interact in this manner and therefore pass through the column more quickly.

In our studies, we are attempting to determine the relative sizes of the bound and unbound scaffolds. If the bound form elutes before the unbound form, then it is likely that the bound form is of a larger size and consists of dimers, trimers, or oligomers. If the bound form

elutes after the unbound form however, then it can be considered *smaller* than the actuator in its open form, and the actuator is most likely closing up into the monomer form.

The molecule used for the gel filtration study was scaffold **7**, and the gel filtration chromatograms are shown below. The eluent used was 7 mM pH 7.2 ammonium acetate buffer with 30% acetonitrile. While every effort was made to ensure that with the choice of eluent there would be no interactions with the column matrix, we discovered that the column has slight ion exchange capability. We therefore washed the column with a 7 mM pH 7.0 EDTA solution containing 30% acetonitrile to remove residual metals before the injection of the unbound actuator and then with a 7 mM pH 7.2 ammonium acetate buffer with 30% acetonitrile and 100 μM $CuCl_2$ to fill up the column's metal-chelating sites before the injection of the bound actuator. This ensured that the unbound actuator would not pick up any metal while in the column and the bound actuator would not lose any metal.

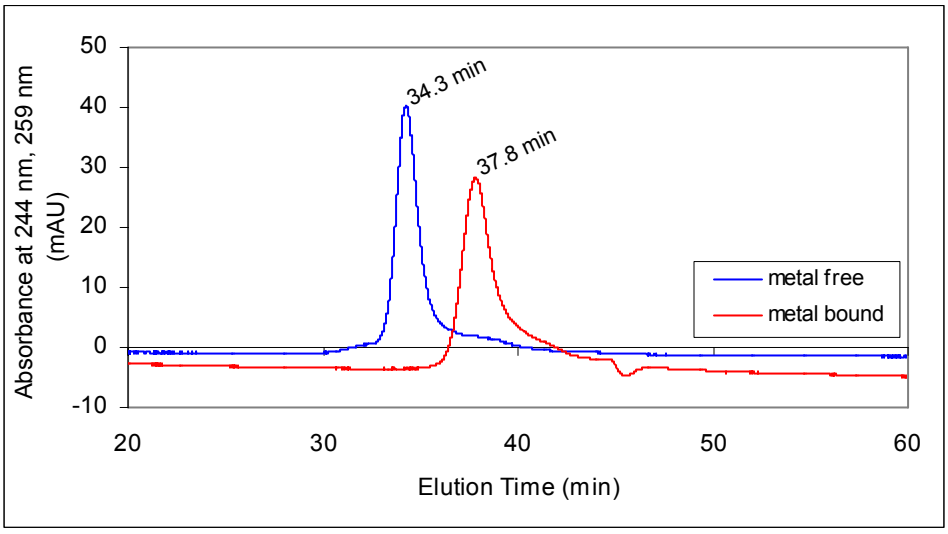

Figure 21: Size exclusion chromatograms of 7 in the metal free state (blue, monitored at 244 nm) and in the presence of one equivalent of $CuCl_2$ (red, monitored at 259 nm).

As seen in Figure 21, the unbound actuator elutes at 34.3 minutes and the copper bound actuator elutes at 37.8 minutes. The metal free vs. metal bound state was determined by measuring the absorption of the peaks (Figure 22).

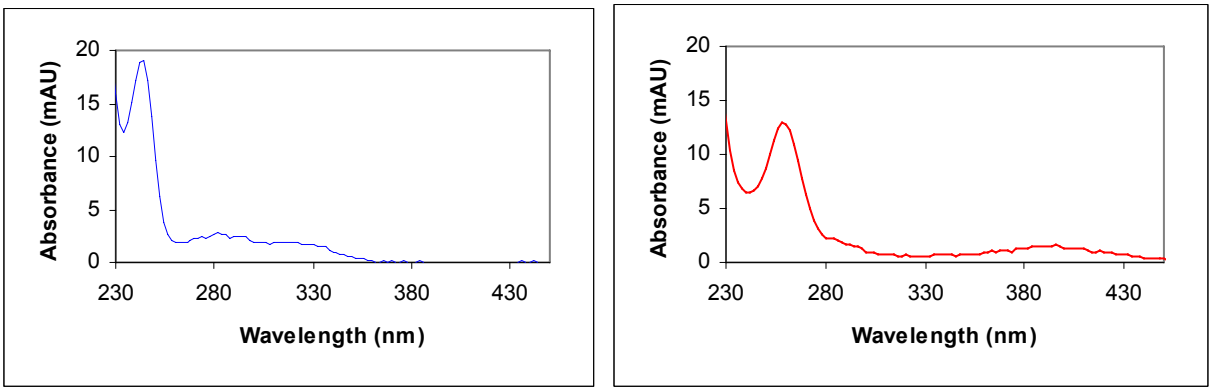

Figure 22: Absorbance spectra of the size exclusion chromatogram peaks of 7, confirming the metal free (34.3 min) and the metal bound (37.8 min) states.

The positive elution time difference confirms that the size of the actuator is in fact decreasing slightly, which supports our hypothesis that the molecule is closing as a monomer rather than in dimers or other higher order structures with the addition of metal. The scale of the time difference, +3.5 minutes, shows how the simple act of binding can greatly affect the overall size and shape of the molecule.

Analytical ultracentrifugation, a classical technique that allows for the measure of molecular weight in solution, is another experiment that can confirm the monomeric nature of the bound actuator. Two types of ultracentrifugation experiments are available: sedimentation velocity, the application of a high centrifugal force and analysis of the time-course of the sedimentation process, and sedimentation equilibrium, the application of low centrifugal force that permits diffusion to balance sedimentation to allow observation of an equilibrium gradient.

A sedimentation equilibrium experiment was performed on both metal free and copper bound samples in 10 mM pH 7.0 phosphate buffer. Using an estimated partial specific volume ($\bar{v}$ = 0.73 mL/g, standard for proteins), the molar mass, M, was determined using the equation below:[26]

$$A = A_0 + \varepsilon_\lambda ce^{\frac{M(1-\bar{v}\rho)(r^2-r_0^2)\omega^2}{2RT}}$$

Two samples of scaffold **7**, metal free at 7 μM, and copper bound at 5 μM were spun at 60,000 rpm for > 8 h before equilibrium was observed. The absorbance curve (measured at 244 and 255 nm, respectively) from the metal free and metal bound samples are shown below.

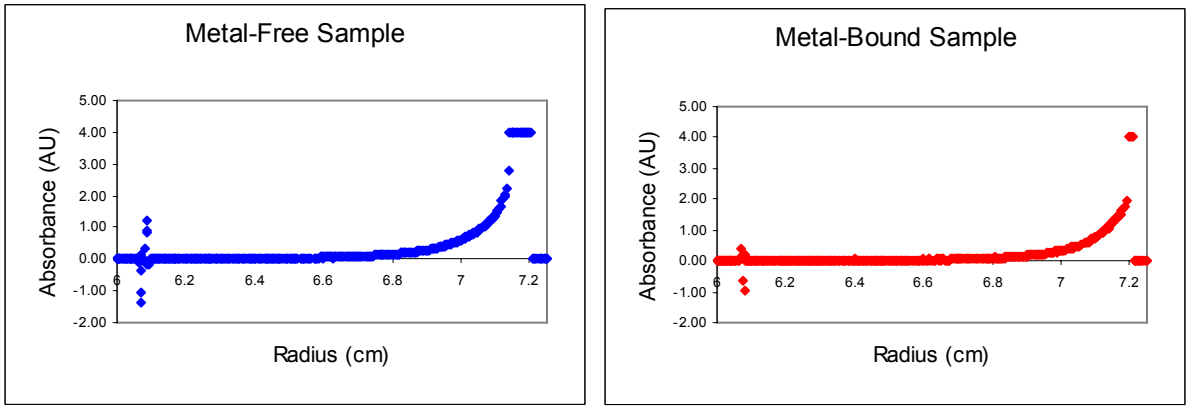

Figure 23: Absorbance curves within the sample cells of 7, in the metal free state and in the presence of metal.

Using the above equation, the molar mass of the metal free was found to be 2400 Da, and the molar mass of the metal bound was found to be 2700 Da. While the mass is 20-30% larger than what is expected from the sequence (1990 Da metal free, 2051 Da metal bound), this is

[26] Wills, P.R.; Winzor, D.J. *Prog. Colloid Polymer Sci.* **2001**, *119*, 113-120.

most likely due to the estimation of $\bar{v}$. The fact that the masses of the metal free and metal bound samples are close to each other implies that the molecule is a monomer in the metal free and metal bound states.

2.4 CONCLUSIONS

We have successfully synthesized a bivalent hinged molecule that binds metal to undergo large conformational changes, similar to an actuator. Spectrophotometric titrations as well as a Job plot have shown that binding occurs on a 1:1 ratio of metal to hinged molecule. Addition of EDTA as a metal scavenger causes the molecule to return to the unbound state. Gel filtration chromatography has shown the effects of metal binding on the overall size and shape of the actuator molecule; the "closed" form is much smaller than the "open" form, indicating that large conformational changes are occurring upon binding. Analytical ultracentrifugation has also unambiguously confirmed that the molecules are binding metal in a monomeric fashion. These results are a first step toward metal-sensing nanovalves and other storage-release type nanosystems.

Another method planned to study the open and closed states of our actuators is to use 2-D electron spin resonance. This technique is capable of measuring exact distances between two unpaired electrons, placed at either end of a molecule. By measuring these large distances, the overall shape of the compound can be inferred.

3.0 EXPERIMENTAL

3.1 GENERAL

Solid phase synthesis was performed in disposable polypropylene reaction columns, connected to a three-way valve equipped with vacuum and argon for mixing. The dichloromethane (DCM) used in coupling reactions was distilled over calcium hydride. The dry grade dimethylformamide (DMF) used in coupling reactions was purchased from Aldrich. Diisopropylethylamine (DIPEA) was distilled under nitrogen sequentially from ninhydrin and potassium hydroxide and stored under molecular sieves. *O*-(7-Azabenzotriazon-1-yl)-*N,N,N',N'*-tetramethyluronium hexafluorphosphate (HATU) was obtained from GenScript. 8-Hydroxyquinoline was obtained from Aldrich. All amino acids and resins were obtained from Novabiochem unless otherwise noted. Pro4(2*S*4*S*) monomer was synthesized using literature procedures.[17] All solid phase reactions were mixed by bubbling argon up through the reactor, allowing for mixing and an inert atmosphere over the reaction.

HPLC-MS analysis was performed on a Hewlett-Packard 1050 HPLC / 1100 electrospray MS instrument equipped with a Waters Xterra MS C_{18} column (3.5 μm packing, 4.6 mm x 100 mm) and a diode-array detector. High resolution ESI-MS was performed on a Waters LC/Q-TOF instrument. Preparative HPLC was performed on a Varian ProStar 500 HPLC system with

an XTerra Prep MS C_{18} column (5 μm packing, 30 mm x 100 mm). UV-Vis experiments were performed on a Varian Cary 50 Bio spectrophotometer in 10 mm quartz cells.

Gel filtration chromatography was performed on a Hewlett-Packard 1050 HPLC instrument equipped with a Superdex Peptide 10/300 GL column (13 μm packing, 10 mm x 300-310 mm).

Analytical ultracentrifugation was performed on a Beckman Optima XL-A / XL-I analytical ultracentrifuge. Data was analyzed using the SEDFIT[27] and SEDNTERP[28] programs.

The concentrations of all solutions of molecules containing **Q** were determined by UV absorption at 25 ºC using the extinction coefficient ϵ_{244} or ϵ_{259} (2 x ϵ_{244} = 56,100 L mol^{-1} cm^{-1}, ϵ_{259} = 49400 L mol^{-1} cm^{-1} determined at pH 7.0 from the slope of the calibration curve A_λ versus concentration). All solutions for Job plots and titrations had concentrations in the micromolar range (10-50 μM) and were prepared in pH 7.0 10 mM phosphate buffer. UV-Vis titrations were carried out by addition of standard metal solutions in water to the titration solution. The absorbance spectra were corrected for dilution and for the absorbance of the metal.

[27] SEDFIT, <http://www.analyticalultracentrifugation.com/default.htm>

[28] SEDNTERP, <http://www.jphilo.mailway.com/download.htm>

3.2 ACTUATOR SYNTHESES

General Solid Phase Peptide Synthesis Procedures:

General Procedure A (HATU coupling):

In a microcentrifuge tube, the amino acid (2 equiv) was dissolved in 20% DCM/DMF (0.2 M) with HATU (2 equiv). After mixing, DIPEA (5 equiv) was added. The solution was left to sit for 10 min activation time, and it was then added to the resin and allowed to react under argon bubbling for 30 min followed by washing with 2 mL each of DCM, *i*-PrOH, DCM for 2 min under argon bubbling. This coupling and washing step was repeated one additional time with the same amino acid.

General Procedure B (Capping):

Unreacted amines are capped by addition of 1 mL of a solution of 50:12.5:1 DMF/Acetic Anhydride/DIPEA with argon bubbling for 20 minutes followed by thorough washing with 2 mL each of DMF, *i*-PrOH, DMF for 2 min under argon bubbling.

General Procedure C (Fmoc Deprotection):

Deprotection of the Fmoc-protected amine is performed by addition of 1 mL of 20% piperidine/DMF followed by argon bubbling for 30 min. The coupling yield can be determined by measuring the absorbance of the piperidine/dibenzofulvene adduct (ε_{301} = 7800 M^{-1} cm^{-1}) in this solution. The resin is then washed thoroughly with 2 mL each of DMF, *i*-PrOH, DMF, *i*-PrOH, and DMF for 2 min each under argon bubbling.

Synthesis of **7**:

A 50 mg batch of hydroxymethyl polystyrene (100-200 mesh) resin (0.98 mmol/g substitution) was transferred to a solid phase reaction vessel. The resin was swollen and the first

amino acid, 42.9 mg *N*-Fmoc-1-napthyl-L-alanine (Acros, 98 μmol), was added to a solution of 1-(mesitylene-2-sulfonyl)-3-nitro-1H-1,2,4-triazole (MSNT), and 1-methylimidazole (MeIm) in DCM and mixed using a micropipettor in a 1.5 mL microcentrifuge tube (5 eq. Amino acid, 5 eq. MSNT, 3.75 eq. MeIm, 0.2 M amino acid in DCM). This solution was added to the resin and allowed to react under argon bubbling for 1 h followed by washing with 2 mL each of DCM, *i*-PrOH, DCM for 2 min under argon bubbling. This coupling and washing step was repeated one additional time with the same amino acid. The sequence was then capped using general procedure B and deprotected using general procedure C.

N_α-Fmoc-N_γ-ivDde-L-diaminobutanoic acid (21.4 mg, 39.2 μmol) was coupled to the resin using the general procedure A, and the sequence was capped using general procedure B and deprotected using general procedure C.

N_α-Fmoc-N_β-Boc pro4(2*S*4*S*) was coupled to the resin using general procedure A. After capping using general procedure B and deprotection using general procedure C, these steps were repeated three more times for this residue, pro4(2*S*4*S*), to give a total of 4 identical residues in a row.

N_α-Fmoc-N_δ-Mtt-L-ornithine (23.9 mg, 39.2 μmol) was coupled to the resin using general procedure A and capped using general procedure B. The deprotection step (general procedure C) however was extended to a total of 2 h to allow for complete diketopiperazine formation. Capping using general procedure B was then repeated, followed by a deprotection of the Mtt group using 1% TFA and 5% TIS in DCM, 10 × 1 mL under argon bubbling. The resin was then neutralized using 5% DIPEA/DCM, 2 × 1 mL under argon bubbling.

N_α-Fmoc-N_β-Boc pro4(2*S*4*S*) was coupled to the resin using the general procedure A. After capping using general procedure B and deprotection using general procedure B, these steps

were repeated three more times for this residue, pro4(2*S*4*S*), to give a total of 4 identical residues in a row.

N_α-Fmoc-N_ε-Mtt-L-diaminopropionic acid (22.8 mg, 39.2 μmol) was coupled to the resin using general procedure A and capped using general procedure B. The deprotection step (general procedure C) was performed for a total of 2 h to allow for complete diketopiperazine formation. The capping step was then repeated, followed by a deprotection of the Mtt group using 1% TFA and 5% TIS in DCM, 10 × 1 mL under argon bubbling. The resin was then neutralized using 5% DIPEA/DCM, 2 × 1 mL under argon bubbling. The *N*-ivDde protecting group on the second residue was then removed using 2% hydrazine in DMF, 10 x 1 mL under argon bubbling. The resin was then washed with 2 mL each of DMF, *i*-PrOH, DMF, *i*-PrOH, and DMF for 2 min each under argon bubbling.

5-Carboxymethyl-8-hydroxyquinoline (19.9 mg, 98 μmol) was coupled using general procedure A, however using 5 equiv acid, 4.8 equiv HATU, 10 equiv DIPEA, 0.2 M in 20% DCM/DMF. The resin was washed with 1 mL of 20% piperidine/DMF under argon bubbling to break up any 8-hydroxyquinoline phenyl ester polymeric chains that had formed on the resin. This coupling and washing step was repeated three additional times. The resin was then prepared for cleavage by washing with 2 mL each of DMF, *i*-PrOH, DMF, *i*-PrOH, DCM, MeOH, DCM, MeOH, and DCM for 2 min. The reactor was then put in a vacuum tube, and dried under reduced pressure overnight.

A small stir bar was added to the solid phase reaction vessel, which was then capped and submerged in an ice bath. Ethanedithiol (12.5 μL) and thioanisole (25 μL) were added followed by TFA (250 μL) and triflic acid (25 μL). The cleavage solution was stirred for 1 h at 0 ˚C and 1 h at room temperature and then filtered dropwise to room temperature ether (15 mL). The resin

was washed with TFA, which was filtered into ether as well. The resulting precipitate was pelleted by centrifugation. The pellet was washed again with ether and dried to a yellow residue using lyophilization. This residue was then dissolved in 20% piperidine/NMP (2 mL) and sealed in an HPLC vial for 36 h with diketopiperazine closure monitored by LCMS. This solution was then added dropwise to ether, and the precipitate was pelleted by centrifugation. The product was purified by preparative HPLC (mobile phase, MeCN (0.05% formic acid) / H_2O (0.1% formic acid), 0% to 50% MeCN over 30 minutes; flow rate 25 mL/min). Desired fractions were concentrated by lyophilization to give a fluffy light yellow solid. The expected mass of **7** was confirmed by HPLC-MS, illustrated in Figure 24 and Figure 25, as well as by high resolution electrospray mass spectrometry (Figure 26-30). The double, triple and quadruple charged species were observed. [HR-MS (ESI) calculated for $C_{95}H_{101}N_{23}O_{25}$ (M+2H)/2: 995.8700, found 995.9069; (M+3H)/3: 664.2493, found 664.2669; (M+4)/4: 498.4389, found 498.4535].

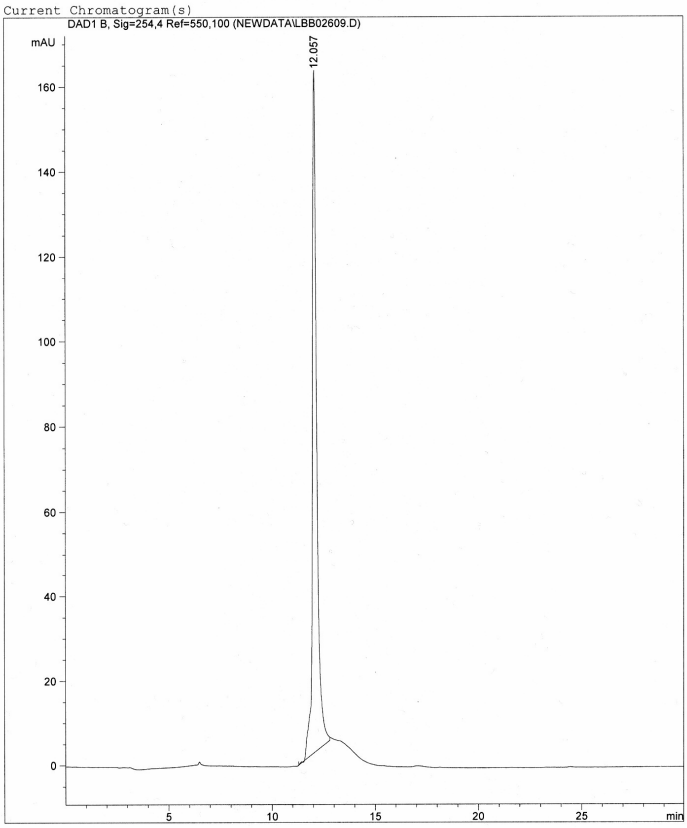

Figure 24: HPLC chromatogram of 7: mobile phase, H2O (0.1% formic acid) / CH3CN, 5% to 50% CH3CN over 30 min; flow rate, 0.80 mL/min; UV detection at 254 nm; tR for 7, 12.1 min.

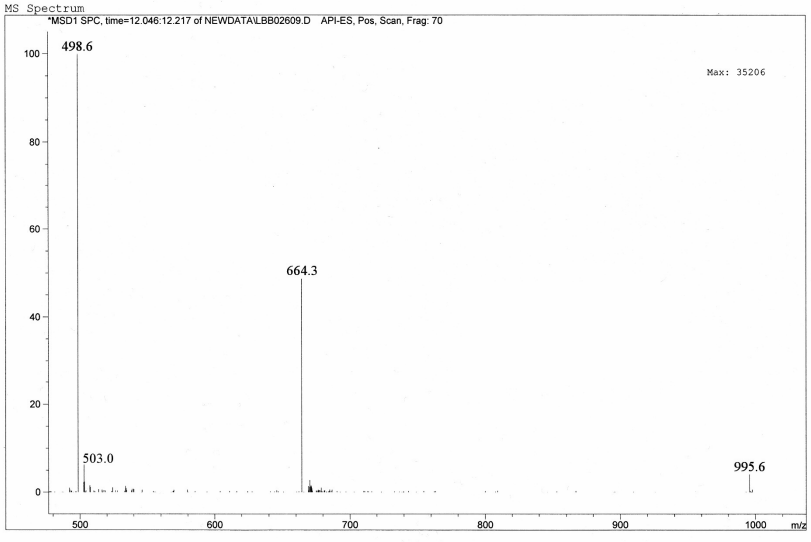

Figure 25: Low resolution mass trace of 7; ESI-MS m/z (ion) 995.6 (M + 2H+)/2, 664.3 (M + 3H+)/3, 498.6 (M + 4H+)/4.

Table 1: Calculated and observed m/z values of 7. Calculation of deviation in ppm between calculated and experimental m/z.

Mass of H	1.0078				
	Calculated m/z	**Experimental m/z**	**delta M**	**Calculation of deviation**	
M	1989.7244				
(M+1)/1	1990.7322				
(M+2H)/2	995.87002	995.9069	0.0369	7.56	ppm
(M+3H)/3	664.2493	664.2669	0.0176	5.41	ppm
(M+4H)/4	498.4389	498.4535	0.0146	5.97	ppm
			Typical deviation of Waters LC/Q-TOF ====>	10	ppm

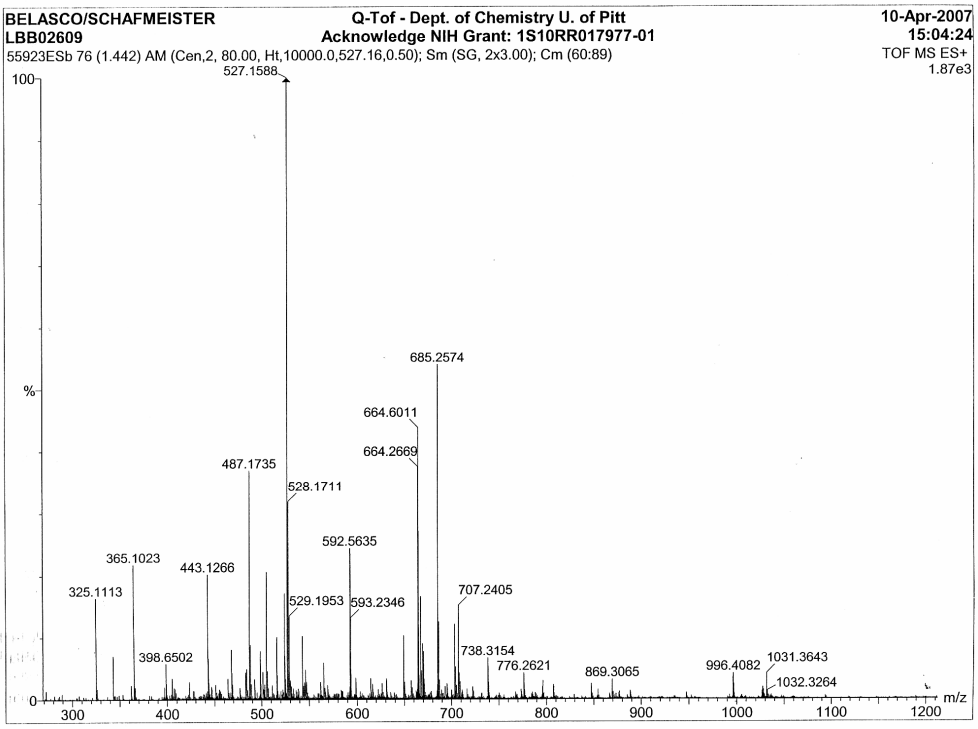

Figure 26: HRMS of 7.

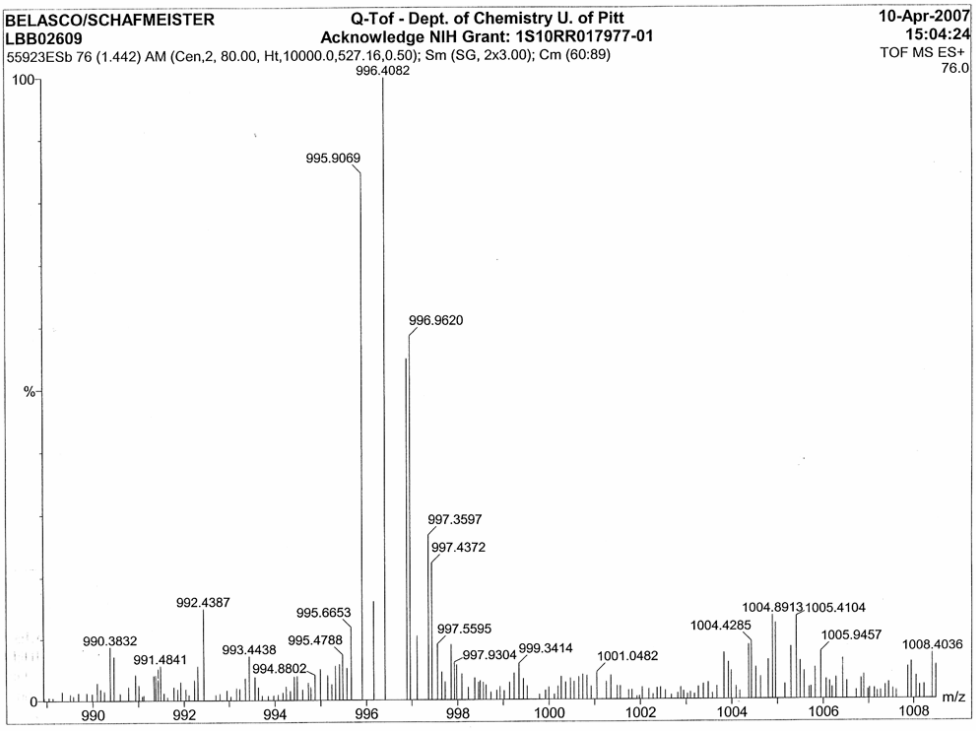

Figure 27: HRMS of (M+2)/2 peak of 7.

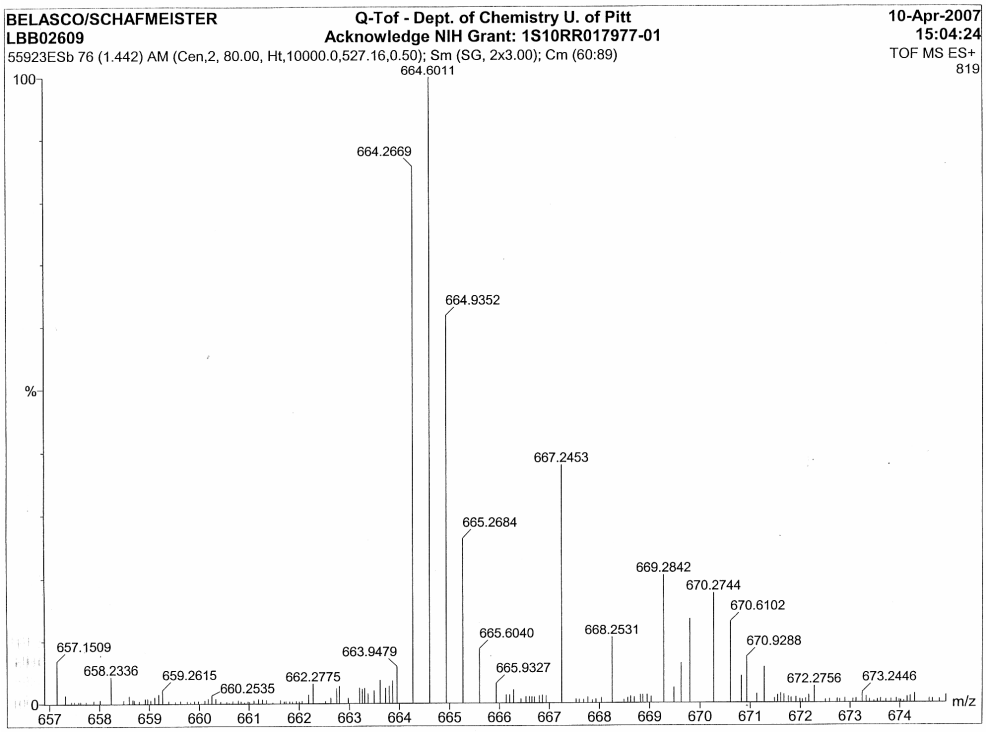

Figure 28: HRMS of (M+3)/3 peak of 7.

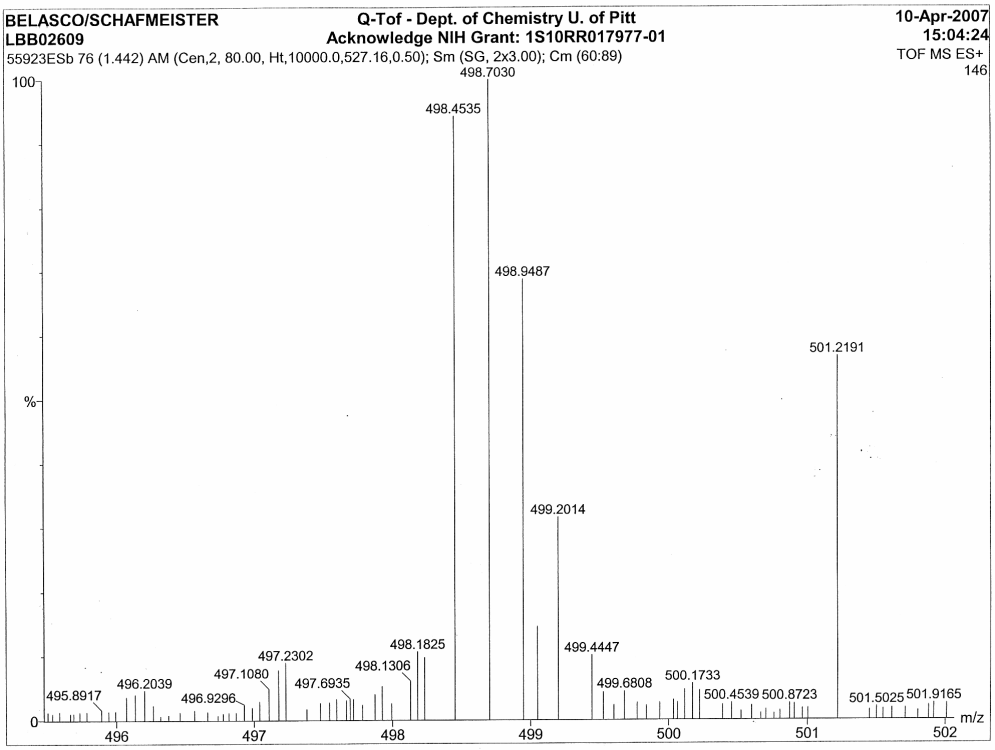

Figure 29: HRMS of (M+4)/4 peak of 7.

Synthesis of **15**

Scaffold **15** was synthesized on a 25 mg scale on the Rink Amide AM (200-400 mesh) resin (0.63 mmol/g substitution). The Fmoc protecting group was removed from the resin linker using general procedure C.

N_α-Fmoc-N_γ-Boc-L-lysine (14.8 mg, 31.5 μmol) was coupled to the resin using general procedure A. After capping using general procedure B and deprotection using general procedure C, these steps were repeated once more for this residue to give a total of 2 identical residues in a row.

N_α-Fmoc-N_γ-ivDde-L-diaminobutanoic acid (17.2 mg, 31.5 μmol) was coupled to the resin using the general procedure A, and the sequence was capped using general procedure B and deprotected using general procedure C.

N_α-Fmoc-N_β-Boc pro4(2S4S) was coupled to the resin using general procedure A. After capping using general procedure B and deprotection using general procedure C, these steps were repeated seven more times for this residue, pro4(2S4S), to give a total of 8 identical residues in a row.

N_α-Fmoc-N_γ-ivDde-L-diaminobutanoic acid (17.2 mg, 31.5 μmol) was coupled to the resin using general procedure A and capped using general procedure B. The deprotection step (general procedure C) was performed for a total of 2 h to allow for complete diketopiperazine formation. The capping step was then repeated, followed by a deprotection of the N-ivDde protecting groups using 2% hydrazine in DMF, 10 × 1 mL under argon bubbling. The resin was then washed with 2 mL each of DMF, *i*-PrOH, DMF, *i*-PrOH, and DMF for 2 min each under argon bubbling.

5-Carboxymethyl-8-hydroxyquinoline (16.0 mg, 78.8 μmol) was coupled using general procedure A, however using 5 equiv acid, 4.8 equiv HATU, 10 equiv DIPEA, 0.2 M in 20% DCM/DMF. The resin was washed with 1 mL of 20% piperidine/DMF under argon bubbling to break up any 8-hydroxyquinoline phenyl ester polymeric chains that had formed on the resin. This coupling and washing step was repeated three additional times. The resin was then prepared for cleavage by washing with 2 mL each of DMF, *i*-PrOH, DMF, *i*-PrOH, DCM, MeOH, DCM, MeOH, and DCM for 2 min. The reactor was then put in a vacuum tube, and dried under reduced pressure overnight.

A small stir bar was added to the solid phase reaction vessel, which was then capped. Water (12.5 μL) and triisopropylsilane (12.5 μL) were added followed by TFA (475 μL). The cleavage solution was stirred for 2 h and then filtered dropwise into a 1.5 mL microcentrifuge tube. The resin was washed with TFA, which was filtered into the microcentrifuge tube as well. The resulting solution was blown dry under nitrogen. This residue was then dissolved in 20% piperidine/NMP (2 mL) and sealed in an HPLC vial for 36 h with diketopiperazine closure monitored by LCMS. This solution was then added dropwise to ether, and the precipitate was pelleted by centrifugation. The product was purified by preparative HPLC (mobile phase, MeCN (0.05% formic acid) / H_2O (0.1% formic acid), 0% to 50% MeCN over 30 min; flow rate 25 mL/min). Desired fractions were concentrated by lyophilization to give a fluffy light yellow solid. The expected mass of **15** was confirmed by HPLC-MS, illustrated in Figure 30 and Figure 31.

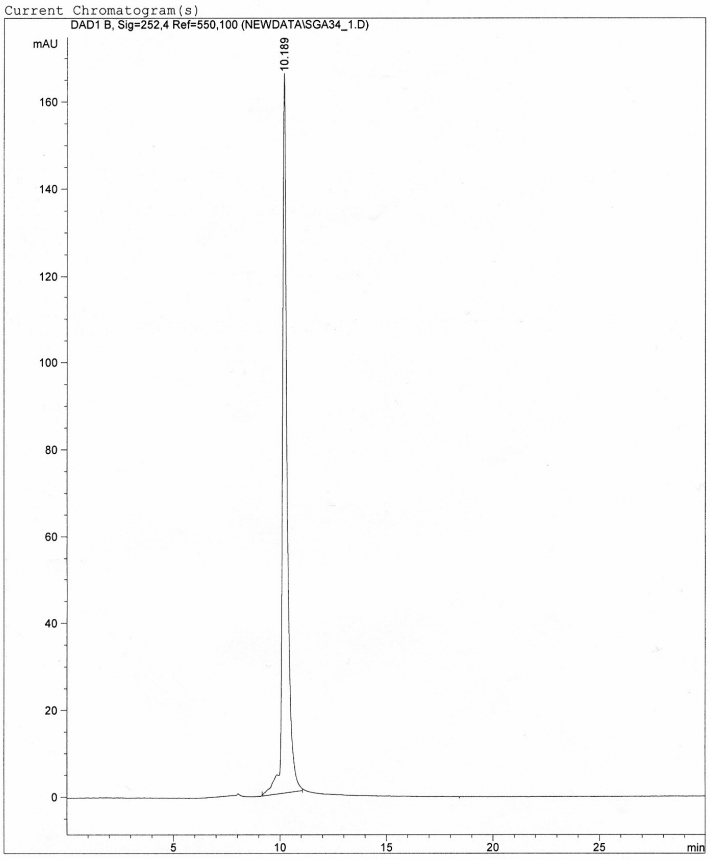

Figure 30: HPLC chromatogram of 15: mobile phase, H_2O (0.1% formic acid) / CH_3CN, 5% to 50% CH_3CN over 30 min; flow rate, 0.80 mL/min; UV detection at 252 nm; t_R for 15, 10.2 min.

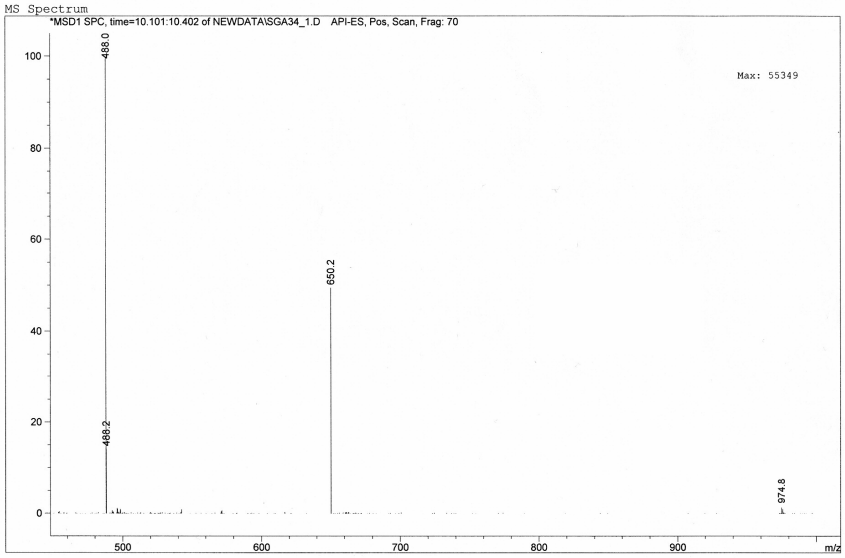

Figure 31: Mass trace of 15; ESI-MS m/z (ion) 974.8 (M + 2H+)/2, 650.2 (M + 3H+)/3, 488.0 (M + 4H+)/4.

BIBLIOGRAPHY

(1) Berg, H. Annular Review of Biochemistry, **2003**, 72, 19-54.

(2) "The History of the Integrated Circuit" www.nobelprize.org

(3) Feynman, R., "There's Plenty of Room at the Bottom," a talk at the annual meeting of the American Physical Society at CalTech, 12/29/59.

(4) Cao, G. Nanostructures & Nanomaterials: Synthesis, Properties & Applications, Imperial College Press, London, 2004.

(5) Bowers, M.J.; McBride, J.R.; Rosenthal, S.J. *J. Am. Chem. Soc.* **2005**, *127*, 15378 – 15379.

(6) Iijima, S. Nature**, 1991,** 354**,** 56-58.

(7) (a) Berber, S.; Kwon, Y.-K.; Tománek, D. Phys. Rev. Lett. **2000**, 84, 4613-4616. (b) Kociak, M.; Kasumov, A.Yu.; Guéron, S.; Reulet, B.; Khodos, I.I. Gorbatov, Yu.B.; Volkov, V.T.; Vaccarini, L.; Bouchiat, H. Phys. Rev. Lett. **2001**, 86, 2416-2419.

(8) Lehn, J.-M. Angew. Chem. Int. Ed. Engl. **1988**, 27, 89.

(9) (a) Tashiro, K.; Konishi, K.; Aida, T. Angew. Chem. Int. Ed. Engl. **1997**, 36, 856-858. (b) Shinkai, S.; Ikeda, M.; Sugasake, A.; Takeuchi, M. Acc. Chem. Res. **2001**, 34, 494-503.

(10) Bosanac, T.; Yang, J.; Wilcox, C.S Agnew. Chem. **2001**, 133, 1927-1931.

(11) Honigfort, M.; Brittain, W. J.; Bosanac, T.; Wilcox, C. S. Macromolecules **2002**, 35, 4849.

(12) Sauvage, J.-P. Acc. Chem. Res. **1998**; 31, 611-619.

(13) (a) Badjic, J.D.; Balzani, V.; Credi, A.; Stoddart, J.F. Science **2004**, 303, 1845-1849. (b) Badjic, J.D.; Ronconi, C.M.; Stoddart, J.F.; Balzani, V.; Silvi, S.; Credi, A. J. Am. Chem. Soc. **2006**, 128, 1489-1499.

(14) Hill, D.J.; Mio, M.J.; Prince, R.B.; Hughes, T.S.; Moore, J.S. Chem. Rev. **2001**, 101, 3893-4011.

(15) (a) Seebach, D.; Abele, S.; Sifferlen, T.; Hänggi, M.; Gruner, S.; Seiler, P. Helv. Chim. Acta **1998,** 81, 2218-2243. (b) Appella, D.H., Barchi, J.J.; Durell, S.R.; Gellman, S.H. J. Am.

Chem. Soc. **1999,** 121, 2309-2310. (c) Kirshenbaum, K.; Barron, A.E.; Goldsmith, R.A.; Armand, P.; Bradley, E.K.; Troung, K.T.V.; Dill, K.A.; Cohen, F.E.; Zuckermann, R.N. Proc. Natl. Acad. Sci. U.S.A. **1998**, 95, 4303-4308. (d) Claridge, T.D.W., Long, D.D.; Hungerford, N.L.; Aplin, R.T.; Smith, M.D.; Marquess, D.G.; Fleet, G.W.J. Tetrahedron Lett. **1999**, 40, 2199-2202. (e) Smith, A.B.; Guzman, M.C.; Sprengeler, P.A.; Keenan, T.P.; Holcomb, R.C.; Wood, J.L.; Carroll, P.J.; Hirschmann, R. J. Am. Chem. Soc. **1994**, 116, 9947-9962. (f) Gude, M.; Piarulli, U.; Potenza, D.; Salom, B.; Gennari, C., Tetrahedron Lett. **1996**, 37, 8589-8592. (g) Hamuro, Y.; Geib, S.J.; Hamilton, A.D. J. Am. Chem. Soc. **1996**, 118, 7529-7541.

(16) Stone, M.T.; Moore, J.S. Org. Lett. **2004**, 6, 469-472.

(17) (a) Levins, C.G.; Schafmeister, C.E. J. Am. Chem. Soc. **2003**, 125, 4702-4703. (b) Habay, S.A,; Schafmeister, C.E. Org. Lett. **2004**, 6, 3369-3371. (c) Gupta, S.; Das, B.C.; Schafmeister, C.E. Org. Lett. **2005**, 7, 2861-2864. (d) Levins, C.G.; Schafmeister, C.E. J. Org. Chem. **2005**, 70, 9002-9008. (e) Levins, C.G.; Brown, Z.Z.; Schafmeister, C.E. Org. Lett. **2006**, 8, 2807-2810.

(18) Levins, C.G.; Schafmeister, C.E. J. Am. Chem. Soc. **2003**, 125, 4702-4703.

(19) (a) Bevan, J.A.; Graddon, D.P.; McConnell, J.F. Nature (London) **1963**, 199, 373. (b) Murray-Rust, P.; Wright, J.D. Inorg. Phys. Theor. **1968**, 247-253. (c) Hoy, R.C.; Morriss, R.H.; Acta Crystallogr. **1967**, 22, 476-482.

(20) (a) Schulman, S.G.; Gershon, H. J. Inorg. Nucl. Chem. **1969**, 31, 2467-2476. (b) Näsänen, R.; Penttinen, U. Acta Chem. Scand. **1952**, 6, 837-843. (c) Richard, C.F.; Gustafson, R.L.; Martell, A.E. J. Am. Chem. Soc. **1959**, 81, 1033-1040. (d) Mellor, D.P.; Maley, L.E. Australian J. Sci. Research **1949**, 2A, 92-110.

(21) Albert, A. Biochem. J. **1953**, 54, 646-654.

(22) Huber, K.P; Herzberg, G., Molecular Spectra and Molecular Structure Constants of Diatomic Molecules, Van Nostrand, New York, 1979.

(23) (a) Watson, R.M.; Skorik, Y.A. Patra, G.K.; Achim, C. J. Am. Chem. Soc. **2005**, 127, 14628-14639. (b) Asher, S.A.; Sharma, A.C.; Goponenko, A.V.; Ward, M.M. Anal. Chem. **2003**, 75, 1676-1683.

(24) (a) Burckhalter, J.H.; Leib, R.I. J. Org. Chem. **1961**, 26, 4078-4083. (b) Warner, V.D.; Sane, J.N.; Mirth, D.B.; Turesky, S.S.; Soloway, B. J. Med. Chem. **1976**, 19, 167-169.

(25) Thanks to Sam Getchell for the synthesis and titration of molecule **15**.

(26) Wills, P.R.; Winzor, D.J. Prog. Colloid Polymer Sci. **2001**, 119, 113-120.

(27) SEDFIT, <http://www.analyticalultracentrifugation.com/default.htm>

(28) SEDNTERP, http://www.jphilo.mailway.com/download.htm